



**HAL**  
open science

# Sunlight Induced Polymerization Photoinitiated by Novel Push–Pull Dyes: Indane-1,3-Dione, 1H-Cyclopenta[b]Naphthalene-1,3(2H)-Dione and 4-Dimethoxyphenyl-1-Allylidene Derivatives

Ke Sun, Corentin Pigot, Yijun Zhang, Timur Borjigin, Fabrice Morlet-savary,  
Bernadette Graff, Malek Nechab, Pu Xiao, Frédéric Dumur, Jacques Lalevée

## ► To cite this version:

Ke Sun, Corentin Pigot, Yijun Zhang, Timur Borjigin, Fabrice Morlet-savary, et al.. Sunlight Induced Polymerization Photoinitiated by Novel Push–Pull Dyes: Indane-1,3-Dione, 1H-Cyclopenta[b]Naphthalene-1,3(2H)-Dione and 4-Dimethoxyphenyl-1-Allylidene Derivatives. *Macromolecular Chemistry and Physics*, 2022, pp.2100439. 10.1002/macp.202100439 . hal-03527019

**HAL Id: hal-03527019**

**<https://hal.science/hal-03527019v1>**

Submitted on 14 Jan 2022

**HAL** is a multi-disciplinary open access archive for the deposit and dissemination of scientific research documents, whether they are published or not. The documents may come from teaching and research institutions in France or abroad, or from public or private research centers.

L'archive ouverte pluridisciplinaire **HAL**, est destinée au dépôt et à la diffusion de documents scientifiques de niveau recherche, publiés ou non, émanant des établissements d'enseignement et de recherche français ou étrangers, des laboratoires publics ou privés.

**Sunlight Induced Polymerization photoinitiated by Novel Push-pull dyes: indane-1,3-dione, 1H-cyclopenta[b]naphthalene-1,3(2H)-dione and 4-Dimethoxyphenyl-1-Allylidene Derivatives**

Ke Sun<sup>1,2</sup>, Corentin Pigot<sup>3</sup>, Yijun Zhang<sup>1,2</sup>, Timur Borjigin<sup>1,2</sup>, Fabrice Morlet-Savary<sup>1,2</sup>, Bernadette Graff<sup>1,2</sup>, Malek Nechab<sup>3</sup>, Pu Xiao<sup>4\*</sup>, Frédéric Dumur<sup>3\*</sup>, Jacques Lalevée<sup>1,2\*</sup>

<sup>1</sup>Université de Haute-Alsace, CNRS, IS2M UMR 7361, F-68100 Mulhouse, France

<sup>2</sup>Université de Strasbourg, France

<sup>3</sup>Aix Marseille Univ, CNRS, ICR UMR 7273, F-13397 Marseille, France

<sup>4</sup>Research School of Chemistry, Australian National University, Canberra, ACT 2601, Australia.

\*Corresponding author: pu.xiao@anu.edu.au (P. X.); [frederic.dumur@univ-amu.fr](mailto:frederic.dumur@univ-amu.fr);

[jacques.lalevee@uha.fr](mailto:jacques.lalevee@uha.fr) (J. L.).

**Abstract:** The free radical polymerization of acrylates photo-initiated by push-pull dye-based photoinitiating systems (PISs) was widely investigated in previous works. As a supplementary investigation on push-pull dyes, here in this article, 25 new push-pull structures comprising electron acceptors derived from indane-1,3-dione and 1H-cyclopenta[b]naphthalene-1,3(2H)-dione (series 1, compounds 1-13) and 4-dimethoxyphenyl-1-allylidene moieties (series 2, compounds 14-25) and various electron donors were synthesized and examined as innovative structures for photoinitiation. Among the twenty-five dyes examined in this work, nine of them (i.e. 2, 3, 5-7, 9, 10, 12 and 13) have never been reported in the literature prior to this work. With the co-initiation of a tertiary amine (ethyl dimethylaminobenzoate EDB) and an iodonium salt and by constituting novel multi-component systems, dyes varying by the

electron-donating groups could efficiently activate photopolymerization both upon irradiation of a light emitting diode (LED) at 405 nm but also with sunlight. Among the two series of dyes examined in this work and by monitoring the polymerization processes by RT-FTIR measurements, four dyes were determined as exhibiting excellent photoinitiation performances and these dyes were selected to perform further studies concerning the chemical mechanisms occurring inside the three-component PISs, e.g. steady state photolysis, fluorescence quenching measurements, and cyclic voltammetry. Then, the electron spin resonance (ESR) spin-trapping experiments were performed to confirm the generated radicals supposed in the discussion part concerning the chemical mechanisms. Markedly, their high photochemical reactivity was also proved by photoinitiation performance upon sunlight. Hence, these results prompt us to develop high performance push-pull dyes as photosensitizers and sunlight could be used as a mild and ecofriendly light source, which can advantageously replace LEDs for the free radical photopolymerization in the future. Finally, the formation of 3D patterns with an excellent gradient of resolution was successfully achieved by the direct laser write (DLW) approach, both for the photopolymerization of photosensitive resins initiated by selected dye-based PISs with/without silica fillers.

**Keywords:** push-pull dye; free radical polymerization; sunlight induced polymerization; LED; 3D printing.

## 1. Introduction

Recently, major developments have been achieved concerning the elaboration of high-performance photoinitiating systems (PISs) by using organic dyes of innovative structures that were not classically used in photopolymerization.<sup>1-5</sup> In this field and among light-harvesting compounds, push-pull dyes comprising an electron-donating group connected to an electron-accepting group have been reported as visible-light sensitive photoinitiators to activate free radical polymerization (FRP).<sup>6-9</sup> Particularly,

due to the existence of the  $\pi$ -conjugated spacer introduced between the electron donor and the electron acceptor, their electron-donating and electron-accepting abilities can be finely tuned, and position of the intramolecular charge transfer (ICT) band extending over the visible range can also be finely controlled too.<sup>10-13</sup> Markedly, the molar extinction coefficients can also be dramatically increased by elongating the length of the  $\pi$ -conjugated spacer. Owing to their attractive features, e.g. high molar extinction coefficients, significant light absorption in the visible range and tunable absorption spectra, various applications could be developed in the presence of the push-pull dye-based PISs.<sup>14-23</sup> Indeed, the uses of push-pull dyes can be given in many fields from organic electronics, e.g. organic light-emitting diodes (OLEDs),<sup>14</sup> organic photovoltaics (OPVs),<sup>15,16</sup> organic-field effects transistors (OFETs),<sup>17</sup> to nonlinear optics (NLO)<sup>18-22</sup> and even waste-water treatment.<sup>23</sup>

In our group, a wide range of chromophores with different push-pull structures has been reported as photoinitiators (PI) upon 405 nm light-emitting diode (LED) and sunlight irradiation.<sup>24-27</sup> Also, intense efforts were devoted noticeably for developing sunlight-induced photopolymerization by using push-pull dye-based PISs.<sup>25-27</sup> In this research field, sunlight exhibits several advantages compared to artificial light produced with a 405nm LED to activate photopolymerization process. Compared to the light emitted from LED, the advantages of sunlight are obvious: broader emission spectrum of the Sun, free and unlimited energy, milder reaction environment, e.g. room temperature.<sup>28-33</sup> Benefiting from these advantages, sunlight may replace the use of artificial light sources with poorer adaption to panchromatic photoinitiators in the future.<sup>34</sup> However, the reported photoinitiator or PISs still suffer from very low reactivity under sunlight for initiating free radical polymerizations. Hence, the intense efforts for developing efficient PIs/PISs with high reactivity are still required. Recently, functional fillers were also used to prepare polymer composites, also constituting an active research field. Indeed, the photopolymerization of resins containing silica fillers fabricated by Direct Laser write (DLW) were successfully achieved in previous researches in our group. As an expectation, this research field was supposed to

constitute a major breakthrough on the knowledge of photopolymerization in material sciences.

Currently, a family of push-pull dyes bearing various structures (See Figure 1) as electron-donating groups and which have never synthesized before, were developed as new photoinitiators to activate the FRP of a benchmark acrylate monomer (TMPTA) under mild light irradiation in this article. In addition, similar to the push-pull dyes comprising the *N*-ethylcarbazole-1-allylidene moiety, a series of push-pull dyes with 4-dimethoxyphenyl-1-allylidene moieties as electron donors was also investigated as supplementary research (series 2, compounds 14-25 in Figure S1). Here, two new families of push-pull dyes were used to prepare three-component photoinitiating systems with co-initiators, i.e. an iodonium salt and a tertiary amine (ethyl dimethylaminobenzoate EDB). Among the different structures, several dyes e.g. dyes 7, 9, 11, 20 proved to be excellent photoinitiators in FRP and could furnish high final acrylate function conversions and short photoinitiation times upon both LED and sunlight irradiation; the polymerization profiles were monitored by Real-Time Fourier Transform Infrared spectroscopy (RT-FTIR). Moreover, the chemical mechanisms of the different PISs and the photochemical properties of the selected push-pull dyes were systematically investigated by steady state photolysis and fluorescence approaches. The proposed mechanisms happening upon sunlight irradiation were also confirmed by using electron spin resonance (ESR) spin-trapping technique. The results indicate that the use of sunlight can constitute an efficient way to replace the energy-consuming LEDs in FRP. For further applications, the new chromophores were successfully used to print 3D patterns with remarkable spatial resolutions by the direct laser write (DLW) approach, even to fabricate photocomposites comprising silica fillers.

## 2. Materials and Methods

### 2.1. Dyes

Chemical structures of dyes 1-13 and 4-dimethoxyphenyl-1-allylidene derivatives

(dyes 14-25) reported in this article are presented in the Figure 1 and in Figure S1, respectively. The synthetic procedures enabling to access to these chromophores are depicted in Section 3.1 and their characterizations are reported in supporting information.

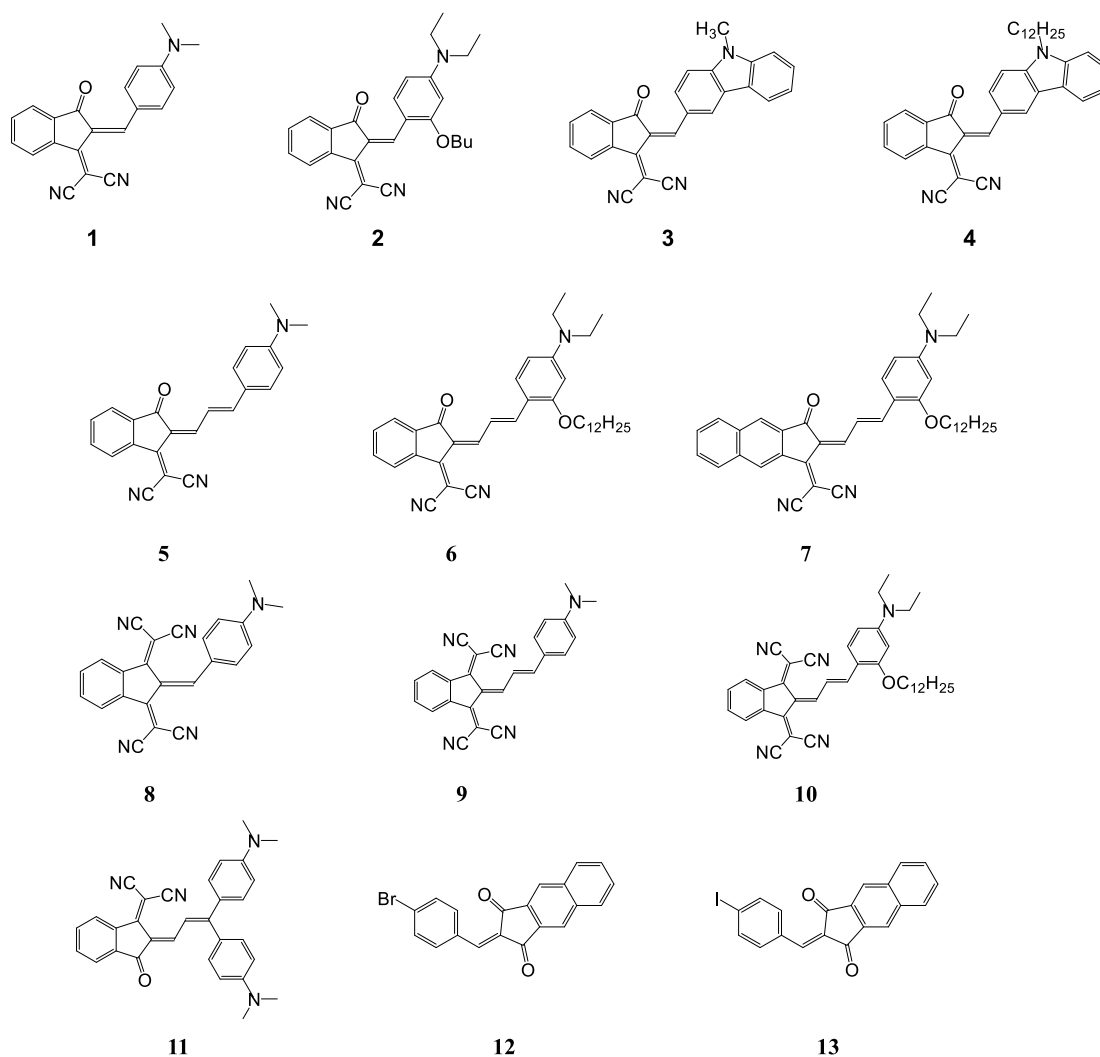


**Figure 1.** Chemical structures of dyes **1-13** used in this study.

## 2.2. Other Materials

In this article, a commercial iodonium salt (marked as Iod - Speedcure 938) was used as co-initiator and an amine (ethyl dimethylaminobenzoate - EDB) was used as the electron donor. Their corresponding chemical structures are shown in Figure 2. Both of these two chemicals were purchased from Sartomer-Lambson Ltd (UK). Also, two kinds of benchmark acrylate monomers (TMPTA and TA) were used in this article, and

their corresponding molecular structures are also depicted in Figure 2. Here, the monomers were purchased from Allnex. Particularly, all the synthetic approaches toward polymerization process reported in this work abided by Green chemistry, given in mild conditions e.g. solvent-free and mild light irradiation conditions (405 nm LED and sunlight) at room-temperature.

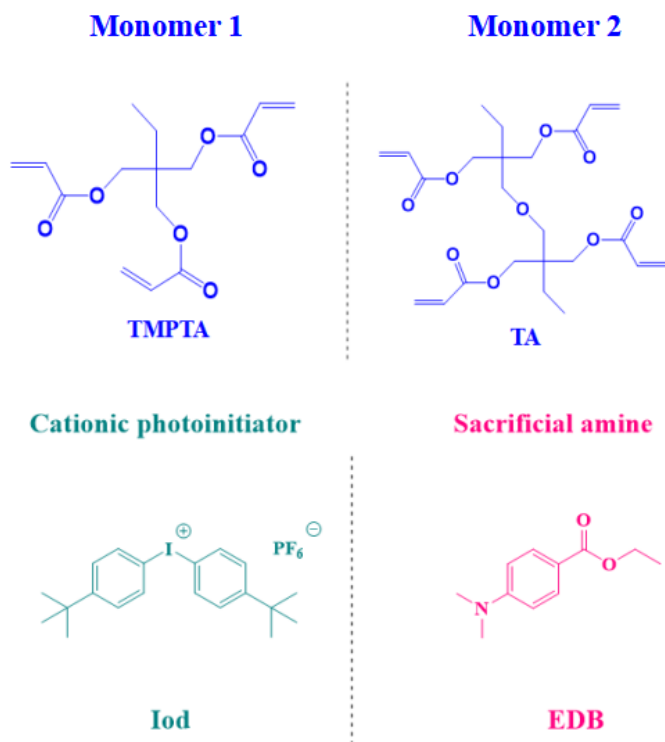


**Figure 2.** Chemical structures of iodonium salt (Iod), the amine (EDB) and the benchmark acrylate monomers (TMPTA and TA) used in this study.

### 2.3. Polymerization profiles obtained by Real Time Fourier Transformed Infrared Spectroscopy (RT-FTIR)

The two families of push-pull dyes were separately dissolved with the iodonium salt (Iod) and the amine (EDB) in benchmark monomers (trimethylolpropane triacrylate noted TMPTA for dyes 1-13; tetrafunctional polyether acrylate noted TA for 4-dimethoxyphenyl-1-allylidene derivatives, dyes 14-25). Also, their weight content ratios in monomer (TMPTA or TA) are: dye/Iod/EDB= 0.1%/2%/2% w/w/w. Then, 1 or 2 drops of prepared photosensitive formulations were deposited in laminate between

2 polypropylene films to control the thickness at  $\sim 100 \mu\text{m}$ . After that, the Free Radical Polymerization (FRP) were activated by exposing the formulations upon irradiation of a LED emitting at 405 nm ( $I_0 = 30 \text{ mW}\cdot\text{cm}^{-2}$ ) or sunlight at mild condition, e.g. room temperature and under air. During the irradiation, the polymerization kinetics was investigated by using real-time FTIR spectroscopy (JASCO FTIR 4100), which can continuously monitor the acrylate functionality at  $\sim 6160 \text{ cm}^{-1}$  to build the polymerization profiles, using the following equation between conversion and irradiation time (eq 1):<sup>35-38</sup>

$$\text{conversion (\%)} = (A_0 - A_t)/A_0 \times 100 \quad (\text{eq 1})$$

where  $A_0$  is the initial peak area before irradiation and  $A_t$  is the peak area after irradiation for a given time  $t$ .

#### 2.4. The chemical mechanisms studies

Investigation of the potential chemical mechanisms in the three-component PISs during photopolymerization is a crucial goal in our works. Here, the steady state photolysis experiments were carried out by using a UV-visible absorption spectroscopy (JASCO V730 UV-visible spectrometer) and a JASCO FP-6200 spectrofluorimeter was used for fluorescence approaches. Moreover, as an important chemical parameter, the Stern-Volmer coefficients ( $K_{sv}$ ) could be obtained from the slopes of Stern-Volmer treatment in fluorescence quenching experiments. Then, the electron transfer quantum yields ( $\phi_{et}$ ) can be calculated according to following equation (eq 2):<sup>36, 37</sup>

$$\phi_{et} = K_{sv}[\text{additive}]/(1+K_{sv}[\text{additive}]) \quad (\text{eq 2})$$

Furthermore, cyclic voltammetry experiments were addressed to investigate oxidation potential (noted  $E_{ox}$ ) and reduction potential (noted  $E_{red}$ ) as the redox potentials of selected dyes. Their redox potentials,  $E_{ox}$ ,  $E_{red}$ , and singlet excited state energy level ( $E_{S1}$ ) could contribute to the calculation of the free energy change from the singlet state ( $\Delta G_{Iod}^{S1}$  or  $\Delta G_{EDB}^{S1}$ ) in the electron transfer reaction according to equations 3 and 4.<sup>39</sup> Here, the singlet excited state energy level ( $E_{S1}$ ) was obtained from the



crossing point of the UV-visible and fluorescence spectra. When replace singlet excited state energy level ( $E_{S1}$ ) by the triplet state energy level ( $E_{T1}$ ) extracted from molecular energy level calculations (Gaussian 03 suite of programs), the free energy change from the triplet state ( $\Delta G_{et}$ ) could also be calculated by equations 5 and 6.<sup>39</sup> Finally, the reduction potential of the iodonium salt and the oxidation potential of EDB could be given by existing literature data, which were reported as  $-0.7 \text{ V}$ <sup>40</sup> and  $1.0 \text{ V}$ <sup>41</sup>, respectively.

$$\Delta G_{\text{Iod}}^{\text{S1}} = E_{\text{ox}} - (-0.7) - E_{\text{S1}} \quad (\text{eq 3})$$

$$\Delta G_{\text{EDB}}^{\text{S1}} = 1 - (E_{\text{red}}) - E_{\text{S1}} \quad (\text{eq 4})$$

$$\Delta G_{\text{Iod}}^{\text{T1}} = E_{\text{ox}} - (-0.7) - E_{\text{T1}} \quad (\text{eq 5})$$

$$\Delta G_{\text{EDB}}^{\text{T1}} = 1 - (E_{\text{red}}) - E_{\text{T1}} \quad (\text{eq 6})$$

Finally, the supposed chemical mechanisms could be proved by detecting radicals  $\text{Ar}^\bullet$  and  $\text{EDB}^\bullet_{(-\text{H})}$  released from Iod and EDB during photolysis in Electron Spin Resonance-Spin Trapping experiments. Here, dye/Iod or dye/EDB were dissolved in *tert*-butylbenzene at a weight content ratio 0.2 mg/mL for dyes and 2 mg/mL for Iod (or EDB). As the spin trap agent, *N-tert*-butyl-phenylnitron (PBN) was also dispersed in the solution at a weight content ratio, 2 mg/mL. Then, the prepared solutions were degassed by saturating the solutions with nitrogen gas at room temperature. During the light irradiation process (LED or sunlight), the radicals were monitored by X-band spectrometer (Bruker EMXplus) and the ESR spectra simulations were carried out using PEST WINSIM software.<sup>36, 37</sup>

## 2.5. Photocomposites preparation

In this work, a weight content of 20% silica powders was dispersed in photosensitive formulations to build the photocomposites containing silica fillers. Formulations were prepared by dissolving dyes, Iod and EDB at the weight contents in the monomer (TMPTA or TA): dye/Iod/EDB, 0.1w%/2%/2%, same as Part 2.3) to

constitute the three-component systems at room temperature and under air.

## **2.6. Direct Laser Write experiments (DLW)**

Photosensitive formulations containing acrylate monomers (TMPTA or TA), PISs (or PISs/silica) were dropped onto a 2 mm-thick homemade tank and then irradiated upon a computer-controlled laser diode@405 nm with spot size around 50  $\mu\text{m}$ . To observe the precise shapes of the fabricated tridimensional patterns, a numerical optical microscope (DSX-HRSU, OLYMPUS corporation) was used after performing the direct laser write on the formulations.

## **2.7. Computational procedure**

Geometry optimizations were performed at the UB3LYP/6-31G\* level. Geometries were frequency checked and the molecular orbitals (MOs) involved in these transitions were extracted.<sup>42, 43</sup>

# **3. Results and Discussions**

## **3.1. Synthesis of the different dyes**

In order to modify the position of the absorption maxima and in order to facilitate the synthesis of the push-pull dyes, several approaches have been considered. Indeed, fine tuning of their panchromatic behavior may imply the modification of the donor or the acceptor moieties but also an elongation of the spacer introduced between the two partners.<sup>44</sup>

During the last decades, the most popular way to tune the position of the absorption maxima of push-pull dyes consisted in modifying the electron donating part, while keeping the same electron acceptor. It allows, by using easily accessible aldehydes to adjust the position of the highest occupied molecular orbital (HOMO) of the push-pull without drastically impacting the position of the lowest unoccupied molecular orbital (LUMO). Moreover, an extension of the spacer may be considered, as in the case of

D4, D5 or D7 (see Figure 3) allowing to redshift the absorption spectra.

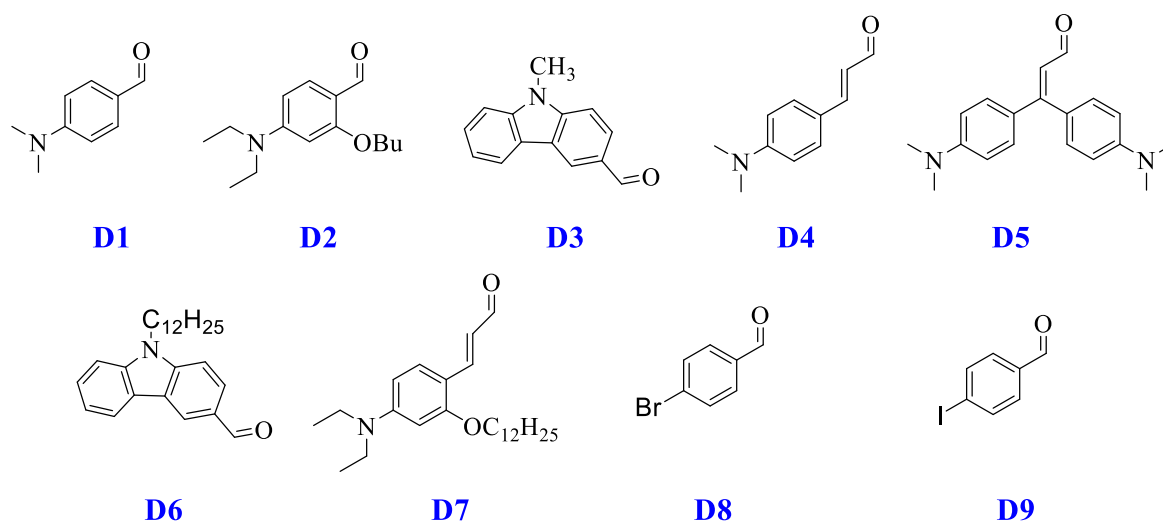
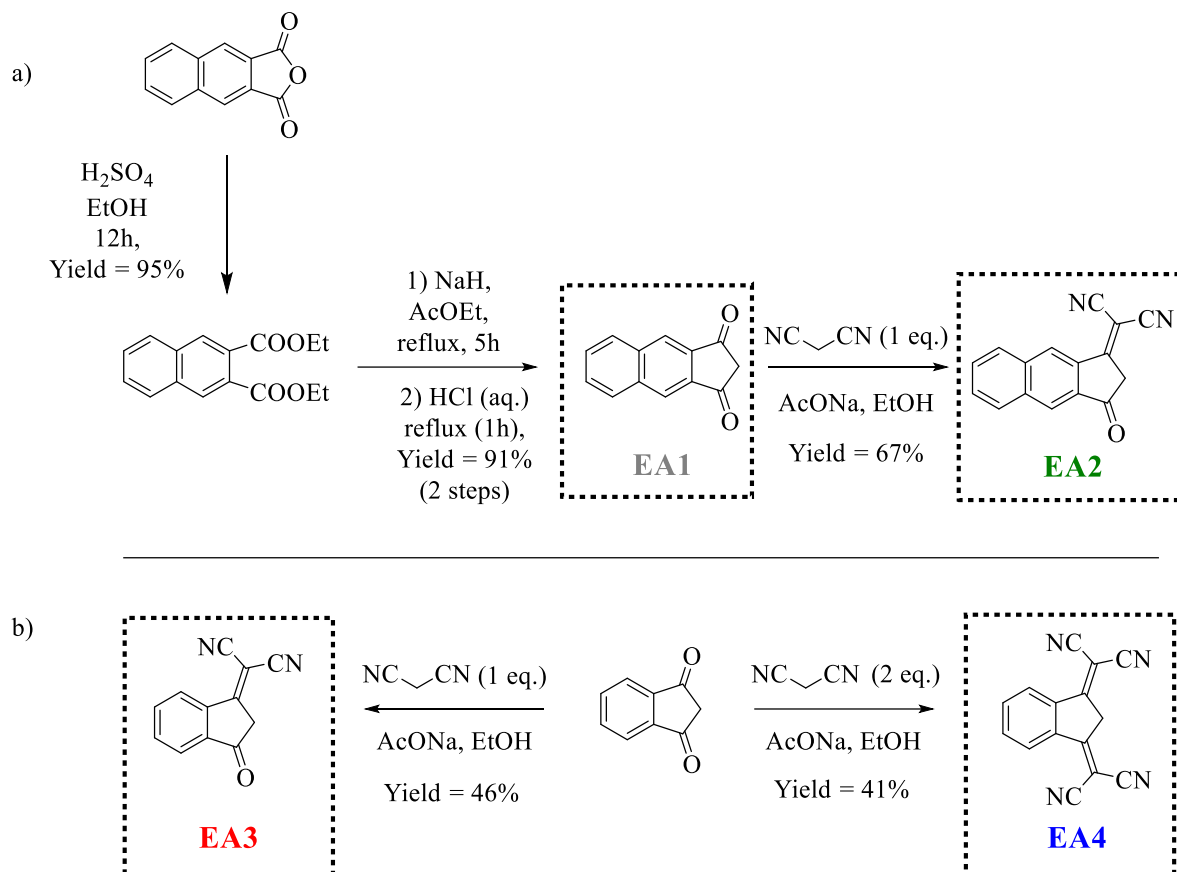


**Figure 3.** Chemical structures of the aldehydes D1-D7 used in this study.

Additionally, this study also considered another approach to design push-pull dyes: the modification of the acceptor moiety. To get access to panchromatic push-pull dyes, we chose to modify a commercially available electron acceptor, namely indane-1,3-dione. Its modifications are already described in the literature but poorly used in photopolymerization.<sup>25</sup>

First, an extension of the aromaticity of the acceptor moiety might also be considered. Indeed, by extending the aromaticity of the electron acceptor, a bathochromic shift of the absorption spectra compared to the parent structures can be anticipated. In this extent, the synthesis of naphthaleneindane-1,3-dione (EA1) (i.e. 1*H*-cyclopenta[*b*]naphthalene-1,3(2*H*)-dione) was performed by a Claisen condensation followed by a decarboxylation in acidic media allowing to get the electron acceptor in 91% yield for the two steps (See scheme 1 a).

Another strategy to improve the electron accepting properties of indane-1,3-dione consists in substituting the carbonyl groups by functions of improved electron-withdrawing ability and a common strategy consists in functionalizing the carbonyl groups by malononitrile. One or two malononitrile groups can be selectively introduced by Knoevenagel condensation, allowing the synthesis of EA2, EA3 and EA4, as shown in the scheme 1.



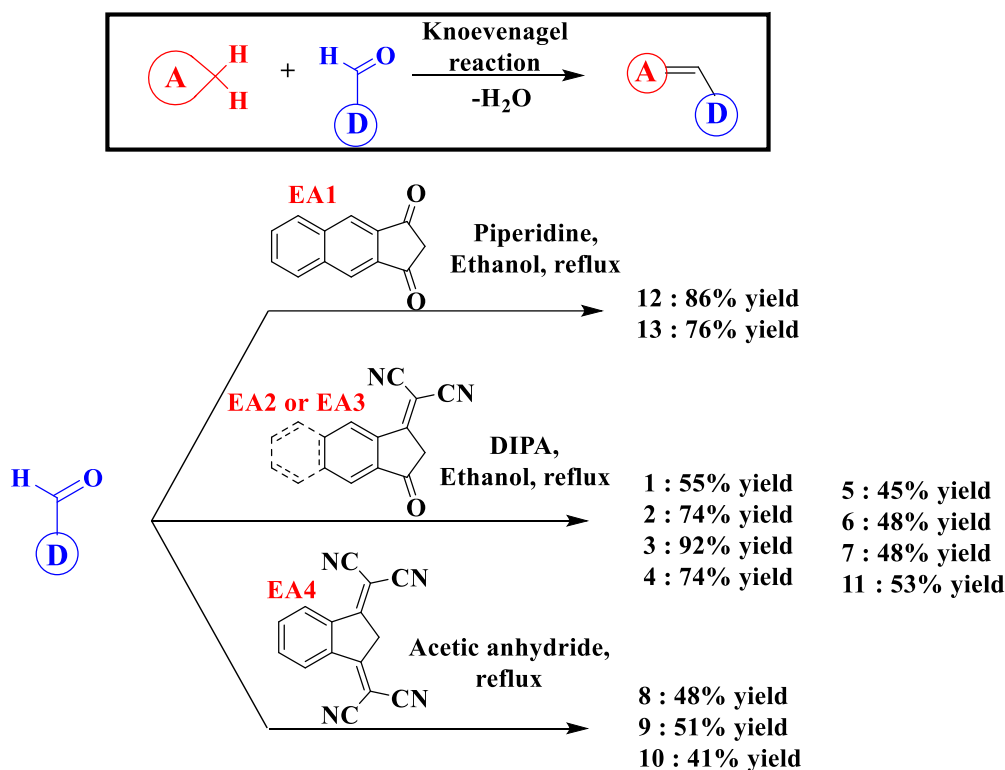
**Scheme 1.** Synthetic routes to electron acceptors a) EA1 and EA2 and b) modification of indane-1,3-dione enabling to produce EA3 and EA4.

Among the different synthesis giving access to push-pull dyes, the Knoevenagel condensation is one of the most popular reaction. Indeed, it allows a simple reaction between an acidic compound, i.e. electron acceptor moiety, with an aldehyde, containing the electron donating moiety.

At the end of the reaction often carried out in alcohol, the product, in most cases, can be recovered by a simple filtration, and obtained in pure form without any further purification. However, some adjustments had to be made depending on the electron acceptor. Indeed, use of EA2 and EA3 as electron acceptors implied the use of diisopropylethylamine (DIPA) i.e. a non-nucleophilic base in order to prevent its addition onto the push-pull dyes. Indeed, addition of a nucleophilic base onto push-pull dyes is notably known to produce azafluorenone by cycloaddition reactions.<sup>45, 46</sup> Also, in order to synthesize dyes 8-11, the Knoevenagel reaction needs to be performed with

an acidic catalyst such as anhydride acetic. Indeed, the intermediate formed by EA4 in a basic media is too stable, imposing these specific reaction conditions for this electron acceptor.

Nonetheless, the Knoevenagel condensation enabled the synthesis of multiple dyes shortly. Being an easy-to-handle reaction, this reaction was selected as the appropriate reaction to synthesize the molecules investigated in this study (See Scheme 2).



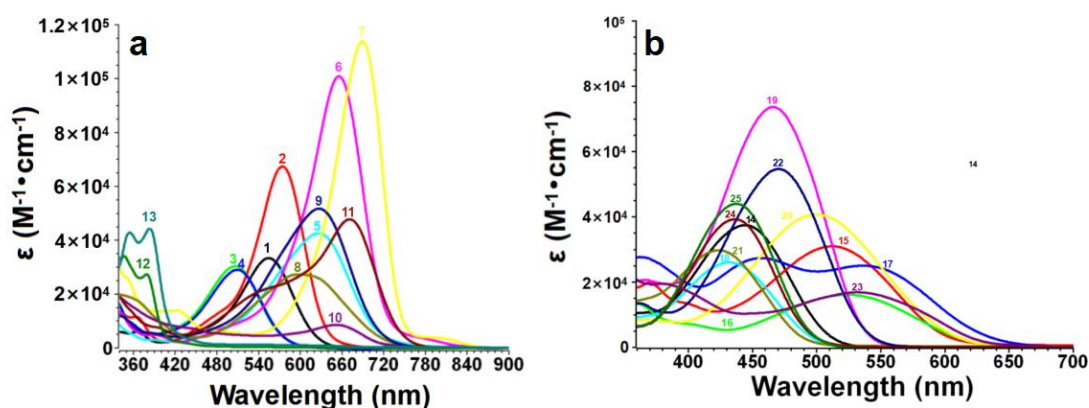
**Scheme 2.** Synthetic routes to dyes 1-11.

It has to be noticed that among the twenty-five dyes examined in this work, dyes 2, 3, 5-7, 9, 10, 12 and 13 have never been reported in the literature. If, the syntheses of dyes 1 and 8, dye 4, dye 11, and dyes 14-25 have previously been reported in the literature, these molecules were never examined as photoinitiators of polymerization, irrespective of the polymerization conditions.

### 3.2. Light absorption properties of the push-pull dyes

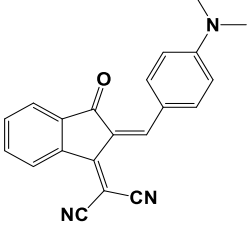
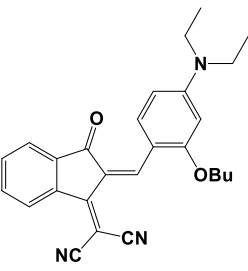
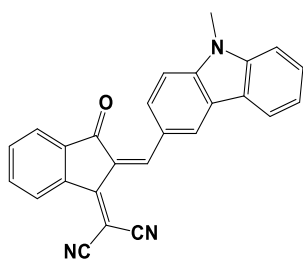
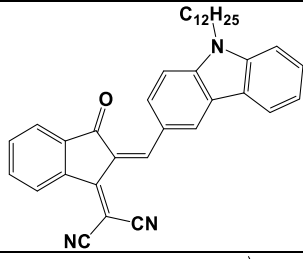
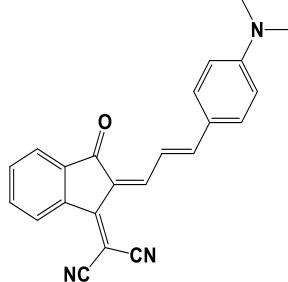
To study the light absorption properties of both series of dyes (series 1-13 in Figure 1 and series 14-25 in Figure S1), molar extinction coefficients ( $\epsilon_{\max}$ ) at both the maximum absorption wavelengths ( $\lambda_{\max}$ ) and at 405nm ( $\epsilon_{405\text{nm}}$ ) were determined by UV-visible absorption spectroscopy. UV-visible absorption spectra of dyes 1-13 are

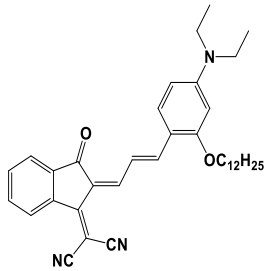
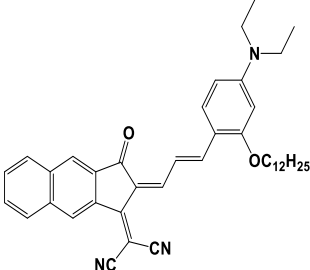
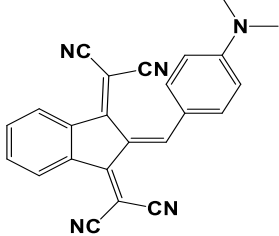
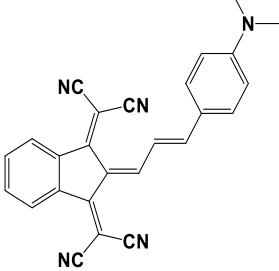
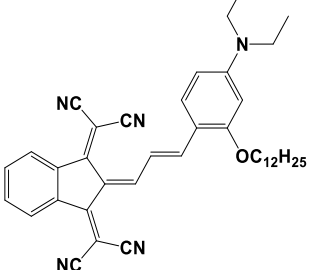
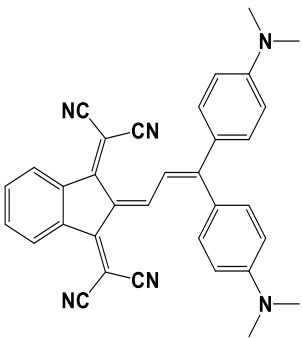
presented in Figure 4a. Absorption spectra of dyes 14-25 are shown in Figure 4b. Light absorption properties ( $\epsilon_{\max}$  and  $\epsilon_{405\text{nm}}$ ) of the different dyes are gathered in the Table 1. Light absorption properties of 4-dimethoxyphenyl-1-allylidene derivatives (dyes 14-25) were reported in the Table 14 of a previous review.<sup>47</sup> Interestingly, based on their absorption properties, dyes 1-25 could be divided into three classes based on the values of their maximum molar extinction coefficients ( $\epsilon_{\max}$ ): (1) the first class which possesses the best light absorption abilities.  $\epsilon_{\max}$  values are greater than  $60000 \text{ M}^{-1}\cdot\text{cm}^{-1}$ , comprising dyes 2, 6, 7, 13, 19; (2) The second class exhibited lower light absorption abilities than that of the previous group, ranging from  $40000 \text{ M}^{-1}\cdot\text{cm}^{-1}$  to  $60000 \text{ M}^{-1}\cdot\text{cm}^{-1}$  which were found in the cases of dyes 5, 9, 11, 20, 22, 25. (3) Finally, for the third class (e.g. dyes 1, 3, 4, 8, 10, 12, 14, 15, 16, 17, 18, 21, 23, 24) molar extinction coefficient were determined as being low, lower than  $40000 \text{ M}^{-1}\cdot\text{cm}^{-1}$ . Considering that the photoinitiation abilities of photoinitiators in the photopolymerization process are directly related to their light absorption abilities, photoinitiating ability were mostly examined for dyes belonging to the two first classes of dyes i.e. classes 1 and 2 as mentioned above.



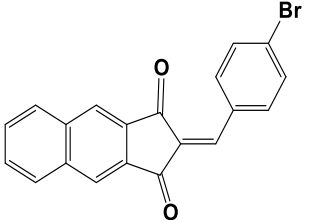
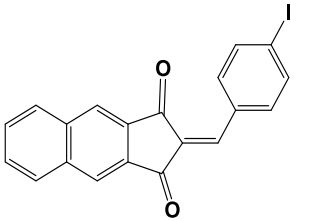
**Figure 4.** UV-visible absorption spectra in acetonitrile of the push-pull dyes (dyes 1-25).

**Table 1.** Newly developed push-pull dyes applicable in PISs. The final function conversion of two-component photoinitiating system without dye (Iod/amine) was cited as blank.

	Push-pull dyes	Absorption properties	Final Acrylate Function Conversion (TMPTA)
1		$\lambda_{\max} \sim 555\text{nm}$ $\epsilon_{\max} \sim 33360 \text{ M}^{-1}\text{cm}^{-1}$ $\epsilon_{405\text{nm}} \sim 2030 \text{ M}^{-1}\text{cm}^{-1}$	<b>~70% @405 LED</b>
2		$\lambda_{\max} \sim 575\text{nm}$ $\epsilon_{\max} \sim 67380 \text{ M}^{-1}\text{cm}^{-1}$ $\epsilon_{405\text{nm}} \sim 2280 \text{ M}^{-1}\text{cm}^{-1}$	<b>~98% @405 LED</b>
3		$\lambda_{\max} \sim 507\text{nm}$ $\epsilon_{\max} \sim 30290 \text{ M}^{-1}\text{cm}^{-1}$ $\epsilon_{405\text{nm}} \sim 5850 \text{ M}^{-1}\text{cm}^{-1}$	<b>~94% @405 LED</b>
4		$\lambda_{\max} \sim 510\text{nm}$ $\epsilon_{\max} \sim 29010 \text{ M}^{-1}\text{cm}^{-1}$ $\epsilon_{405\text{nm}} \sim 5570 \text{ M}^{-1}\text{cm}^{-1}$	<b>~80% @405 LED</b>
5		$\lambda_{\max} \sim 626\text{nm}$ $\epsilon_{\max} \sim 42550 \text{ M}^{-1}\text{cm}^{-1}$ $\epsilon_{405\text{nm}} \sim 2550 \text{ M}^{-1}\text{cm}^{-1}$	<b>~98% @405 LED</b>

6		$\lambda_{\max} \sim 656\text{nm}$ $\epsilon_{\max} \sim 100870 \text{ M}^{-1}\text{cm}^{-1}$ $\epsilon_{405\text{nm}} \sim 3880 \text{ M}^{-1}\text{cm}^{-1}$	~62% @405 LED
7		$\lambda_{\max} \sim 689\text{nm}$ $\epsilon_{\max} \sim 113870 \text{ M}^{-1}\text{cm}^{-1}$ $\epsilon_{405\text{nm}} \sim 13640 \text{ M}^{-1}\text{cm}^{-1}$	~97% @405 LED ~93% @sunlight
8		$\lambda_{\max} \sim 598\text{nm}$ $\epsilon_{\max} \sim 27290 \text{ M}^{-1}\text{cm}^{-1}$ $\epsilon_{405\text{nm}} \sim 8310 \text{ M}^{-1}\text{cm}^{-1}$	~61% @405 LED
9		$\lambda_{\max} \sim 627\text{nm}$ $\epsilon_{\max} \sim 51700 \text{ M}^{-1}\text{cm}^{-1}$ $\epsilon_{405\text{nm}} \sim 4610 \text{ M}^{-1}\text{cm}^{-1}$	~98% @405 LED ~91% @sunlight
10		$\lambda_{\max} \sim 650\text{nm}$ $\epsilon_{\max} \sim 8570 \text{ M}^{-1}\text{cm}^{-1}$ $\epsilon_{405\text{nm}} \sim 8950 \text{ M}^{-1}\text{cm}^{-1}$	~85% @405 LED
11		$\lambda_{\max} \sim 671\text{nm}$ $\epsilon_{\max} \sim 47770 \text{ M}^{-1}\text{cm}^{-1}$ $\epsilon_{405\text{nm}} \sim 6560 \text{ M}^{-1}\text{cm}^{-1}$	~99% @405 LED ~92% @sunlight



12		$\lambda_{\max} \sim 379\text{nm}$ $\epsilon_{\max} \sim 27320 \text{ M}^{-1}\text{cm}^{-1}$ $\epsilon_{405\text{nm}} \sim 5120 \text{ M}^{-1}\text{cm}^{-1}$	~98% @405 LED
13		$\lambda_{\max} \sim 384\text{nm}$ $\epsilon_{\max} \sim 44320 \text{ M}^{-1}\text{cm}^{-1}$ $\epsilon_{405\text{nm}} \sim 15420 \text{ M}^{-1}\text{cm}^{-1}$	~93% @405 LED

### 3.3. Photopolymerization kinetics with the newly proposed push-pull dyes in three-component photoinitiating systems

To investigate the photoinitiation behaviors of the newly proposed push-pull dyes, light-induced photopolymerization was performed in the presence of push-pull dye-based three-component systems, comprising an iodonium salt as the electron acceptor, and a tertiary amine (ethyl dimethylaminobenzoate EDB) as the electron donor. As the benchmark acrylate monomer (TMPTA for dyes 1-13, TA for dyes 14-25 due to their poor solubility/photoinitiation abilities in TMPTA), acrylate function conversions upon irradiation with a 405 nm LED during the FRP were monitored by Real-Time Fourier Transform Infrared spectroscopy (RT-FTIR) at room temperature. For push pull dyes alone, no polymerization occurs showing the huge role of the EDB and Iod additives on the polymerization performance.

Photopolymerization profiles initiated by dyes 1-13 are presented in Figure 5a, and their final acrylate function conversions (FCs) after 400 s of irradiation are gathered in the Table 1. Markedly, we set the same weight ratios of co-initiators, Iod and EDB, for all dye-based PISs, which were kept at 2% Iod and 2% EDB in monomer (TMPTA), while the content of different dyes was kept at a same weight ratio, 0.1% in monomer. Moreover, a reference system (2% Iod: 2% amine in TMPTA) without dyes was used to give a better comprehension on the dye-based PIS. Polymerization profile and final

function conversion obtained with this reference system are also shown in Figure 5a and Table 1, cited as dye 0 for TMPTA, or identified as blank. For the blank, the initiation ability comes from the formation of photosensitive Iod-amine charge transfer complexes.<sup>47</sup> From the different results, remarkable acrylate function conversions were obtained obviously in the cases of dyes 7, 9, 11-based PISs (~97%~99%), which possess better photoinitiation abilities than the reference system that only reached 60% in TMPTA. Interestingly, polymerization profiles of dyes 7, 9, 11-based PISs showed short induction periods ( $T-T_0$  with T: Start time of polymerization;  $T_0$ : Start time of light irradiation). Markedly, the polymerization initiated by dye 7-based PIS was extremely fast, since the maximum monomer conversion could be obtained within 20 s. Conversely, the other dye-based PISs exhibited poorer photoinitiation abilities, characterized by lower final acrylate function conversions or longer induction periods. In this context, we selected dyes 7, 9, 11 to investigate the free radical photopolymerizations of TMPTA under sunlight irradiation and for the following steady state experiments.

Sunlight photopolymerization experiments were carried out with the following weather conditions, under weak solar illumination and environment (around ~21°C) at 14:00-16:00 pm on 9<sup>th</sup>, July 2021, in Mulhouse Area (+77° 43' E, -47° 75' N) of France. As shown in Figure 5b, three selected push-pull dyes exhibited high performance during the polymerization of TMPTA under sunlight irradiation, furnishing high final reactive function conversions (FCs): ~99% for dye 7 (black curve), ~95% for dye 9 (red curve), ~92% for dye 11 (blue curve), proving their high photoinitiation abilities under natural light source as efficient photoinitiators. Obviously, dye 7 demonstrated a higher final conversion (~90%) under sunlight compared to that of dyes 5 and 6. Dye 9 furnished the lowest final conversion, only reaching 90%.

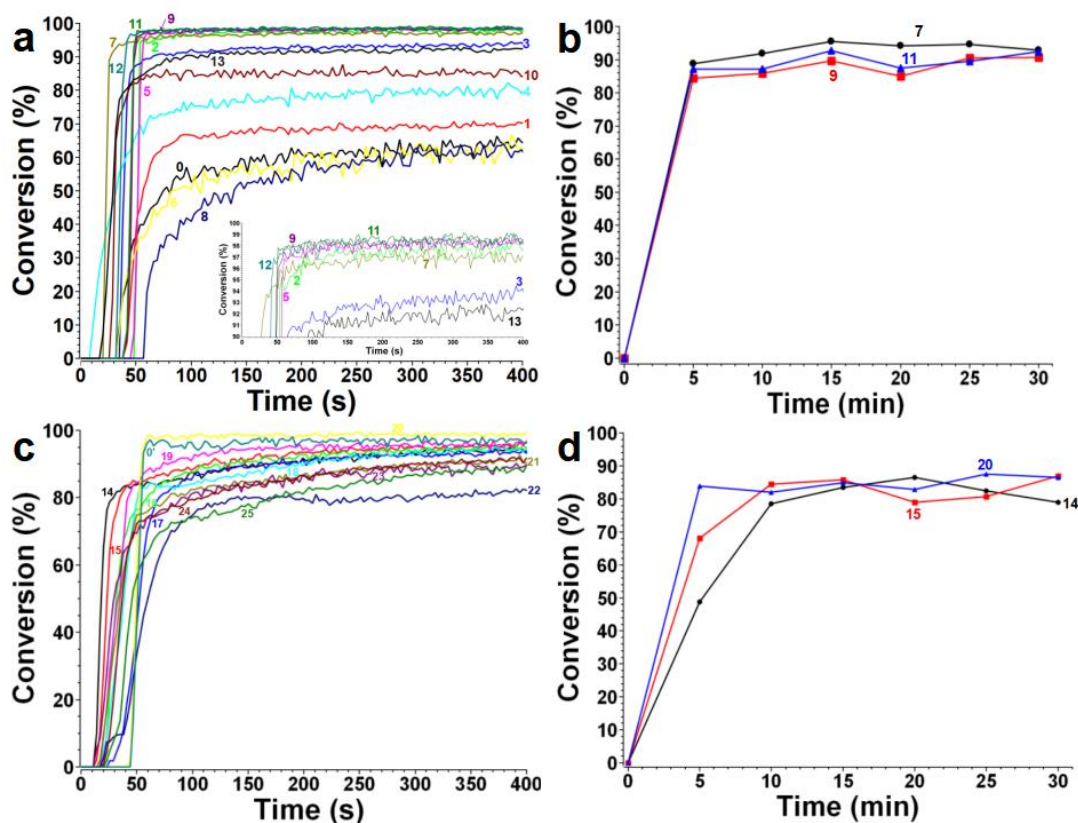


**Figure 5.** (a) Photopolymerization profiles of TMPTA (conversion of C=C bonds vs irradiation time) initiated by an iodonium salt and EDB upon exposure to LED@405nm in laminate in the presence of dyes 1-13 at the same weight ratio: dye:Iod:EDB = 0.1%:2%:2% in TMPTA. Curve 0: Iodonium salt: EDB=2%:2% in TMPTA without dye. (b) Photopolymerization profiles of TMPTA (conversion of C=C bonds vs irradiation time) initiated by the iodonium salt and EDB upon exposure to sunlight in laminate in the presence of dyes at the weight ratio: dye:Iod:EDB=0.1%:2%:2% in TMPTA. (black) dye 7; (red) dye 9; (blue) dye 11. (c) Photopolymerization profiles of TA (conversion of C=C bonds vs irradiation time) initiated by an iodonium salt and EDB upon exposure to LED@405nm in laminate in the presence of dyes 14-25 at the same weight ratio: dye:Iod:EDB = 0.1%:2%:2% in TA. Curve 0': Iodonium salt: EDB=2%:2% in TA without dye. (d) Photopolymerization profiles of TA (conversion of C=C bonds vs irradiation time) initiated by the iodonium salt and EDB upon exposure to sunlight in laminate in the presence of dyes at the weight ratio: dye:Iod:EDB=0.1%:2%:2% in TA. (black) dye 14; (red) dye 15; (blue) dye 20.

In our previous works, push-pull dyes e.g. *N*-ethylcarbazole-1-allylidene derivatives have been evidenced to be efficient light harvesting compounds and their high photoinitiation abilities were examined in free radical polymerization upon sunlight irradiation. The series of push-pull dyes based on 4-dimethoxyphenyl-1-allylidene moieties (14-25) investigated in this article was also examined as

photoinitiators of polymerization under both irradiation with a 405nm LED and sunlight in the same conditions than that used for the previous series based on *N*-ethylcarbazole-1-allylidene derivatives, e.g. contents of dye/Iod/EDB in three-component systems, at the room temperature, etc. Among dyes 14-25, only dye 20 furnished a higher final conversion (~99%) than the reference system in TA (~97%, cited as dye 0' for TA in Figure 5c). Even if this family of push-pull dyes (dyes 14-25 excepted dye 20) showed lower FCs than the reference system or *N*-ethylcarbazole-1-allylidene derivatives with similar chemical structures reported in our previous work, however, their photoinitiation abilities were also established in polymerization profiles in Figure 5c, and their final conversions were listed in the Table 14 of published review<sup>47</sup> to make the investigation more systematically.

Three photopolymerization profiles of TA initiated dyes 14, 15, 20-based PISs upon sunlight are depicted in Figure 5d. Fortunately, high initiation performances were observed for dyes 2 and 7 during the sunlight induced photopolymerization. The two dyes furnished a same high function conversion (FCs): ~87% both for dye 14 (black curve) and dye 20 (blue curve). A lower final conversion was obtained in the case of dye 15 (FC~79%). These results confirm that high photoinitiation abilities can be also achieved upon irradiation with natural light source with this series of dyes.

In conclusion, high photoinitiation abilities can be achieved upon irradiation with sunlight in the presence of the investigated dyes (dyes 1-25) as light harvesting compounds.

### **3.4. Proposed chemical mechanisms**

#### **3.4.1. Steady state photolysis experiments of dye-based Photoinitiating Systems**

Steady state photolysis experiments upon irradiation with a LED at 405 nm were established to investigate the interactions between the three components (dye, Iod and EDB) in newly developed systems by UV-visible spectroscopy. Here, the three dyes, dyes 7, 9, 11 were dissolved in acetonitrile as the organic solvent at concentrations of  $5.26 \times 10^{-6}$  M,  $9.85 \times 10^{-6}$  M,  $7.58 \times 10^{-6}$  M, respectively. Then, the iodonium salts was

introduced at the concentration of  $2.93 \times 10^{-2}$  M and (or) EDB at  $8.15 \times 10^{-2}$  M, were also added to prepare the three-component systems in the solutions. The two-component systems (dye/Iod and dye/EDB) of three selected dyes were also prepared as two partial reactions of the three-component system, while the contents of dye, Iod (or EDB) and the conditions in two-component systems were the same than that used for the three-component systems in order to investigate the chemical mechanisms in detail.

For the dye 7-based systems, an increase of the absorbance in its UV-vis absorption spectra could be detected in the case of dye 7/EDB upon irradiation at 405 nm, whereas an opposite trend was observed for dye 7/Iod/EDB and dye 7/Iod two-component systems (see Figure S2a, b, respectively). Increase of the absorbance upon irradiation is indicative that a new photoproduct was formed in the solution with the dye 7/EDB system during the irradiation process. Considering that a decreasing tendency was observed during the steady state photolysis experiments of the three-component system, we assumed that the generated photoproduct was consumed by the radicals formed by the dye 7/Iod combination. Indeed, investigations on their chemical mechanism will be discussed in the following part 3.4.2.

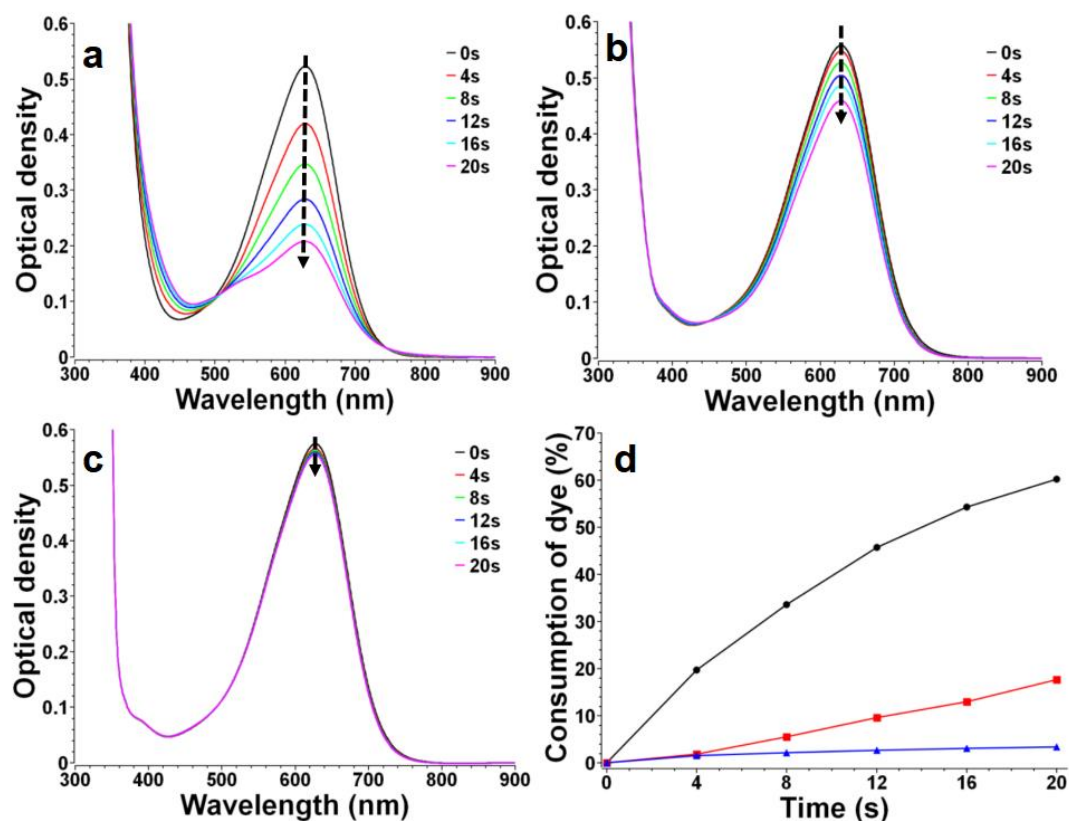


**Figure 6.** UV-visible absorption spectra of dye 9 ( $9.85 \times 10^{-6}$  M) with co-initiators in acetonitrile: **(a)** Iod ( $2.93 \times 10^{-2}$  M) and EDB ( $8.15 \times 10^{-2}$  M), **(b)** Iod ( $2.93 \times 10^{-2}$  M), **(c)** EDB ( $8.15 \times 10^{-2}$  M) upon exposure to LED@405nm under air for different time. **(d)** Consumption of dye 9 vs. irradiation time under the irradiation of LED@ 405 nm: dye 9/Iod/EDB(●); dye 9/Iod(■); dye 9/EDB(▲).

Steady state photolysis experiments of dye 9 and dye 11 were carried out in similar conditions for both the dye-based three-component and two-component systems. From the results depicted in Figure 6 for dye 9 and Figure 7 for dye 11, all of the photolysis procedures including three and two-component systems showed decreasing photolysis process, while the consumption of dye 9 and 11-based three-component systems (~60% for dye 9 and ~48% for dye 11) achieved higher value compared to that observed for the dye/Iod and dye/EDB systems. Also, both the dye 9 and dye 11/Iod (~17.7% for dye 9/Iod, ~31.6% for dye 11/Iod) systems furnished higher consumption than that observed with dye 9 (~3.4% for dye 9/EDB, ~0.8% for dye 11/EDB). Markedly, even if dye/Iod and dye/EDB photolysis processes both contribute to the integrated interactions in the three-component systems, interestingly, dye/Iod interaction gave more contributions

when compared to the dye/EDB interaction, proving the higher efficiency of the dye/Iod combination in free radical polymerization process.

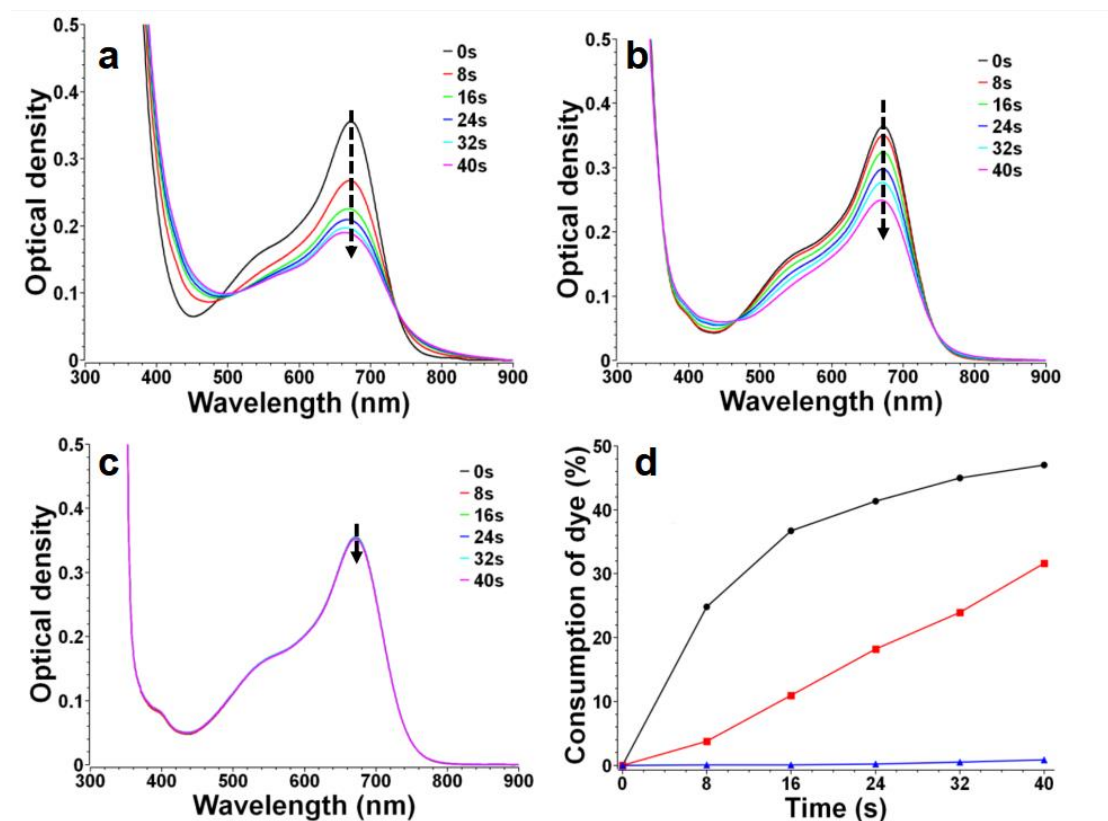


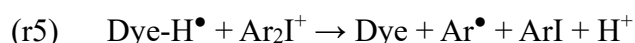
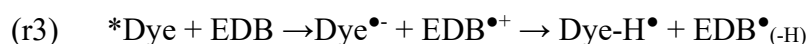
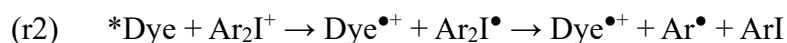
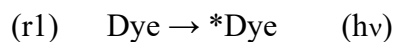
**Figure 7.** UV-visible absorption spectra of dye 11 ( $7.58 \times 10^{-6}$  M) with co-initiators in acetonitrile: (a) Iod ( $2.93 \times 10^{-2}$  M) and EDB ( $8.15 \times 10^{-2}$  M), (b) Iod ( $2.93 \times 10^{-2}$  M), (c) EDB ( $8.15 \times 10^{-2}$  M) upon exposure to LED@405nm under air for different times. (d) Consumption of dye 11 vs. irradiation time under the irradiation of LED@ 405 nm: dye 11/Iod/EDB(●); dye 11/Iod(■); dye 6/EDB(▲).

Finally, dyes 14, 15, 20 were also selected to investigate their steady state photolysis experiments upon irradiation with the LED at 405 nm. Interestingly, the UV-visible absorption spectra exhibited increasing tendencies for all three push-pull dye-based three-component systems during the irradiation process with the 405 nm LED (See Figure S3a, b, c for dyes 14, 15, 20, respectively). These phenomena indicated the same chemical mechanisms occurring in solutions for the three dye-based PISs, for which new photoproducts were generated during the steady state photolysis processes. Hence, we can consider that the formation of the new photoproducts also existed during

the photopolymerization process when using the three-component systems (dye/Iod/EDB) comprising dyes 14, 15, 20 as the photosensitizers. Formation of these photoproducts can also be assumed for the other push-pull dyes based on 4-dimethoxyphenyl-1-allylidene moiety.

### 3.4.2. Proposed chemical mechanisms

Similar to previous researches, the chemical mechanisms occurring with the push-pull dye-based PISs were supposed and divided into two partial reactions: dyes/Iod and dyes/EDB interactions. Indeed, the dyes can react both with Iod or EDB when considered separately. There is a fundamental process to activate the ground states of the dyes then promoted in their excited states (dye\*) upon irradiation in the first step (see r1 in Scheme 3). After that, the oxidation reaction can happen with the dye\*/Iod combination and then generate radicals and Dye<sup>•+</sup> as depicted in r2 reaction. Oppositely, the reduction reaction can occur for the dye\*/EDB interaction and can also generate Dye-H<sup>•</sup> as shown in r3 reaction (see Scheme 3). To finalize the catalytic cycle, the ground state of the dye can be regenerated by further reactions between both Dye<sup>•+</sup>/EDB and Dye-H<sup>•</sup>/Iod interactions as shown in r4, r5 (See Scheme 3), respectively. Particularly, the radicals Ar<sup>•</sup> and EDB<sup>•(-H)</sup> generated from Iod and EDB in reactions r4, r5 can constitute powerful evidences confirming the supposed chemical mechanisms, since the radicals can be detected by ESR-spin trapping experiments. The discussion of the results attained by ESR-spin trapping experiments will present in the following part.



**Scheme 3.** Proposed photoinitiation mechanisms of the dyes/Iod/EDB redox combination.



**Table 2.** Parameters characterizing the chemical mechanisms associated with dyes 7, 9, 11, 20 in acetonitrile.<sup>a, b, c</sup>

	<b>Dye 7</b>	<b>Dye 9</b>	<b>Dye 11</b>	<b>Dye 20</b>
<b>E<sub>S1</sub> (eV)</b>	1.73	1.84	-	2.21
<b>E<sub>T1</sub> (eV)<sup>a</sup></b>	1.41	1.35	1.40	
<b>ΔG<sup>S1</sup><sub>Iod</sub> (eV)<sup>b</sup></b>	-0.29	-0.88	-	-0.05
<b>ΔG<sup>S1</sup><sub>EDB</sub> (eV)<sup>c</sup></b>	0.43	-0.2	-	-0.54
<b>ΔGet<sup>T1</sup><sub>Iod</sub> (eV)<sup>b</sup></b>	0.03	-0.39	0.11	
<b>ΔGet<sup>T1</sup><sub>EDB</sub> (eV)<sup>c</sup></b>	0.75	0.29	0.23	
<b>E<sub>ox</sub> (V)</b>	0.74	0.26	0.81	1.46
<b>E<sub>red</sub> (V)</b>	-1.16	-0.64	-0.63	-0.67

a: calculated triplet state energy level at DFT level.

b: For Iod, the reduction potential of -0.7 V is used according to ref. [40].

c: For EDB, the oxidation potential of 1.0 V is used according to ref. [41].

The singlet excited state energies (E<sub>S1</sub>), calculated from the associated spectra given by normalized UV-visible absorption and normalized fluorescence spectra of dye in acetonitrile can act as powerful tools to evaluate the chemical mechanisms occurring with the dye/Iod and dye/EDB combinations (Figure 8). Here, the crossing point of the two curves could be determined, and the singlet excited state energies (E<sub>S1</sub>) of dyes 7, 9, 20 are gathered in Table 2 after calculation: 1.73 eV for dye 7; 1.84 eV for dye 9; 2.21 eV for dye 20. As exception, there is no fluorescence curve observed for dye 11, therefore, the E<sub>S1</sub> of dye 11 cannot be given as well.

Another experimental parameters, e.g. the oxidation potential (E<sub>ox</sub>), the reduction potential (E<sub>red</sub>) of selected dyes were measured from their electron transfer in acetonitrile characterized by cyclic voltammetry experiments which uses

tetrabutylammonium hexafluorophosphate as the supporting electrolyte. Here, we set the scanning between -2000 and 2000 mV, and their cyclic voltammograms are presented in Figure S4 for dyes 7, 9, 11. As the results, the half peak potentials in oxidation and reduction cyclic could be determined and the data are gathered in Table 2. Additionally, the oxidation and reduction potentials of dye 20 are also given in Table 2:  $E_{ox} = 1.46$  V,  $E_{red} = -0.67$  V.

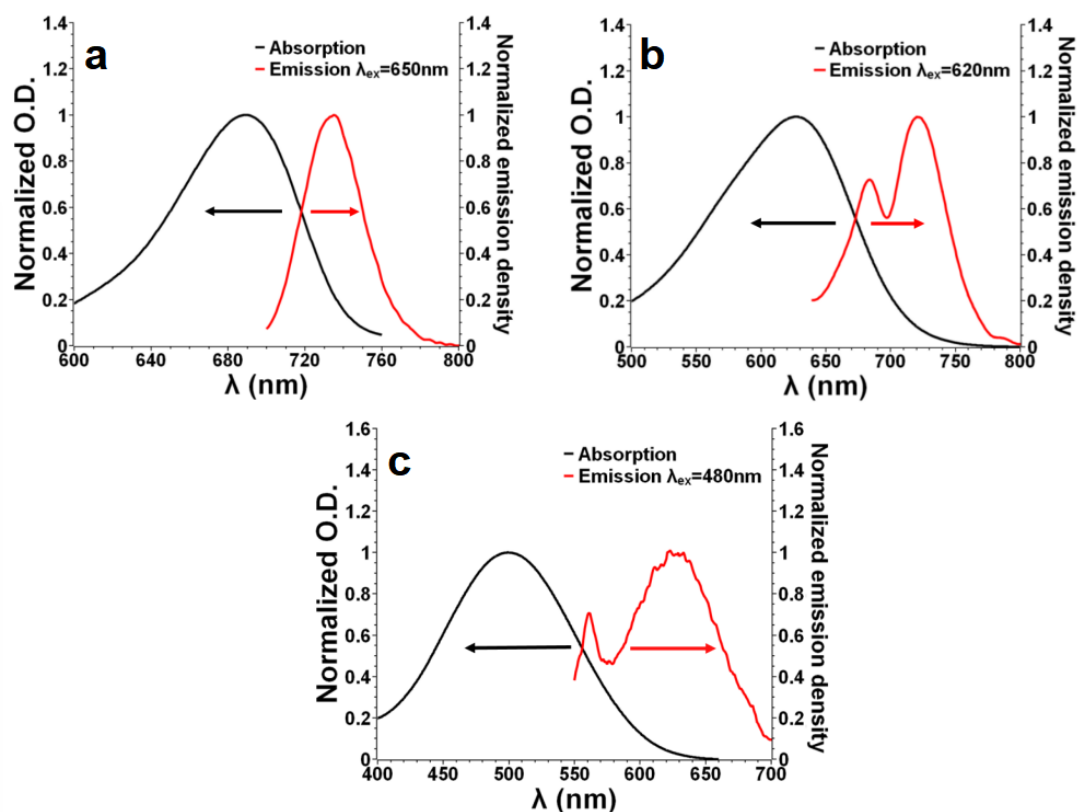


**Figure 8.** Singlet state energy determination in acetonitrile for: (a) dye 7; (b) dye 9; (c) dye 20.

With the aforementioned calculated chemical parameters e.g. oxidation potential ( $E_{ox}$ ), the reduction potential ( $E_{red}$ ) and the singlet excited state energy ( $E_{S1}$ ), the free energy changes  $\Delta G_{Iod}^{S1}$  or  $\Delta G_{EDB}^{S1}$  could be determined and enabled to estimate the feasibility for the electron transfer reaction in dye/Iod and dye/EDB combinations according to equations (eq. 3-6). For dyes 9 and 20, their free energy changes  $\Delta G_{Iod}^{S1}$  or  $\Delta G_{EDB}^{S1}$  were negative suggesting a favorable process e.g.  $\Delta G_{Iod} = -0.05$  eV,  $\Delta G_{EDB} =$

-0.54 eV for dye 20. However, the free energy changes  $\Delta G_{\text{EDB}}^{\text{S1}}$  of dye 7 was positive, even if its  $\Delta G_{\text{Iod}}^{\text{S1}}$  was negative. Additionally, the free energy changes of dye 11 could not be determined as no fluorescence could be detected for dye 11. These results are gathered in Table 2, indicating the theoretical feasibility of the electron transfer reactions in selected dyes. These data are fully consistent with the results given by steady state photolysis.

Calculations of the triplet energy levels  $E_{\text{T1}}$  (eV) of dyes 7, 9, 11, 20 were performed at DFT level, and the data are gathered in Table 2. The triplet routes involved in mechanisms can be ruled out for the dye/EDB interactions due to all of their free energy changes at triplet state  $\Delta G_{\text{et}}^{\text{T1}}$  that are greater than 0, even if the dye 9/Iod interactions looks favorable.

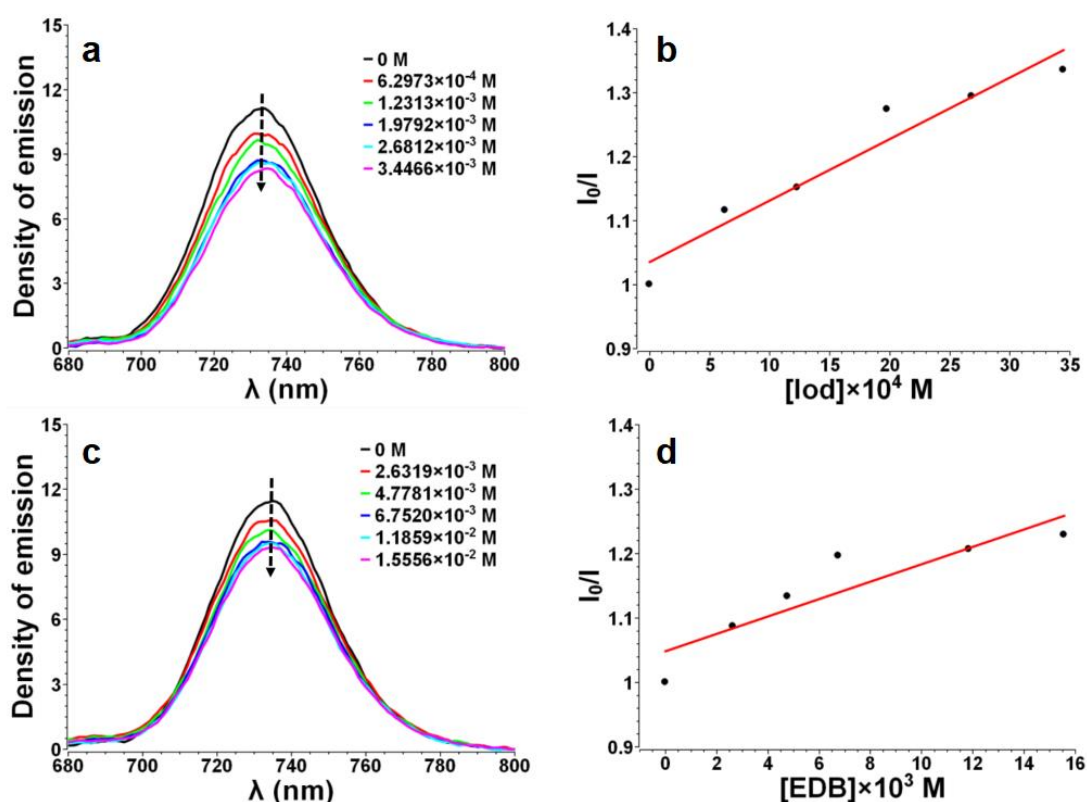


**Figure 9.** Fluorescence quenching of: (a) dye 7 ( $5.26 \times 10^{-6}$  M in acetonitrile) by **iodonium salt (Iod)**; (c) dye 7 ( $5.26 \times 10^{-6}$  M in acetonitrile) by **amine (EDB)**. Stern–Volmer treatment for fluorescence quenching of the (b) dye 7/iodonium; (d) dye 7/EDB.

Notably, the fluorescence quenching experiments on dyes 7, 9, 11, 20 in acetonitrile were also performed to examine the interaction effects between dye and Iod (or EDB). An obvious decline process was detected during the fluorescence quenching experiments both for dye 7/Iod and dye 7/EDB solutions (see Figure 9a for dye 7/Iod, Figure 9c for dye 7/EDB). Moreover, the decline process was also found in the fluorescence quenching of dye 20/Iod and dye 20/EDB combination. Then, the decline processes in fluorescence quenching of dye 7/Iod and dye 7/EDB were treated by using the Stern–Volmer treatment as shown in Figure 9b for dye 7/Iod and Figure 9d for dye 7/EDB. According to eq 2, the Stern-Volmer coefficients  $K_{sv}$  and the electron transfer quantum yields ( $\phi_{et}$ ) could be calculated by the slope of Stern–Volmer treatment. Similarly,  $K_{sv}$  and  $\phi_{et}$  of dye 20/Iod and dye 20/EDB combinations were also determined in the same way (gathered in Table 3).

**Table 3.** Parameters characterizing the fluorescence quenching properties of dye 7 and 20 in acetonitrile: Interaction constant ( $K^{sv}$ ) between dye/Iod and dye/EDB systems calculated by Stern–Volmer equation; electron transfer quantum yield ( $\phi_{et(S1)}$ ) of dye/Iod and dye/EDB interaction.

	$K^{sv}_{Iod}(M^{-1})$	$\phi_{et(S1)_{Iod}}^a$	$K^{sv}_{EDB}(M^{-1})$	$\phi_{et(S1)_{EDB}}^a$
Dye 7	96	0.80	1.84	0.18
Dye 20	15	0.39	9	0.52

### 3.3.4. ESR spin-trapping experiments

To make a clear understanding on the chemical mechanism during the FRP, ESR-spin trapping experiments were performed to confirm the structure of the radicals generated from the dyes/Iod (or EDB) interactions under light irradiation (405nm LED or sunlight) (Figure 10). Here, the dye/Iod (or dye/EDB) two-component PISs and PBN (the spin trap agent), were dissolved into *tert*-butylbenzene at specific weight

concentration ratio ( $[\text{dye}] = 0.2 \text{ mg/mL}$ ;  $[\text{Iod}] = [\text{EDB}] = 2 \text{ mg/mL}$ ;  $[\text{PBN}] = 0.2 \text{ mg/mL}$ ) under Nitrogen as protection gas. The radicals,  $\text{Ar}^\bullet$  and  $\text{EDB}^{\bullet(-\text{H})}$  previously suggested were clearly detected in dye 7, 9, 20/Iod (or EDB) solutions and the ESR spectra of dyes/Iod (or EDB) comprising the curves both measured before and after irradiation of 405 LED are presented in Figure S5 for dye 7, Figure S6 for dye 9 and Figure S7 for dye 20.

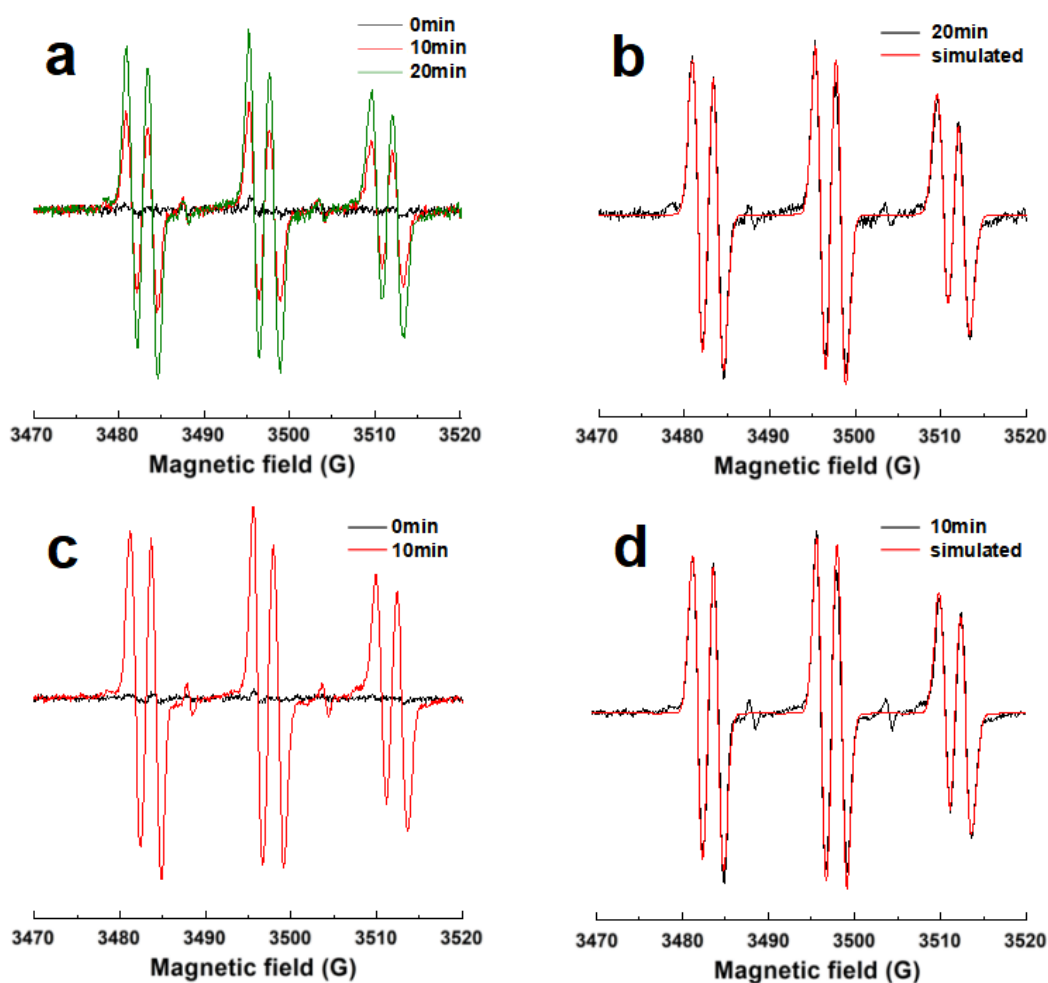


**Figure 10.** ESR spectra obtained from ESR-spin trapping experiments under irradiation of sunlight using  $\text{PBN} = 2 \text{ mg/mL}$  (as the spin trap agent);  $\text{Iod} = 2 \text{ mg/mL}$ ,  $\text{EDB} = 2 \text{ mg/mL}$  and  $\text{dye 11} = 0.2 \text{ mg/mL}$  in *tert*-butylbenzene under  $\text{N}_2$ . (a) **dye 11/Iod PIS**, Irradiation time = 20 min (green) = 10 min (red) and = 0 min (black) spectra, respectively; (b) **dye 11/Iod PIS**, Irradiation time = 20 min experimental (black) and simulated (red) spectra; (c) **dye 11/EDB PIS**, Irradiation time = 10 min (red) and = 0 min (black) spectra; (d) **dye 11/EDB PIS**, Irradiation time = 10 min experimental (black) and simulated (red) spectra.

However, ESR-spin trapping experiments under sunlight irradiation were also performed on dyes 11 and 20, as reliable results to compare with that obtained under 405nm LED. Here, the ESR curves attained before and after sunlight irradiation are characterized and illustrated in Figures 10-11. Interestingly, obvious enhancement of the ESR curves were observed in the case of dye 11/Iod and dye 11/EDB (see Figure 10), which are quite different to the results obtained with the 405nm LED. Moreover, the supposed radicals were also generated in dye 20/Iod (dye 20/EDB) combination under sunlight irradiation (see Figure 11), even if an elongated irradiation time was required, around 15 min compared to that under irradiation of 405nm LED. Markedly, the ESR-spin experiments irradiated by sunlight mentioned above were performed around 2:00 pm on 9<sup>th</sup>, July, 2021, in Mulhouse Area (+77° 43' E, -47° 75' N) of France, and the weather conditions were illustrated in Figure S8.

As a confirmation of the existing radicals, the Hyperfine Couplings Constants (HFC) for the PBN radical adducts were also determined by ESR spectra simulation. Finally, the HFCs determined by ESR-spin experiments for the dyes 7, 9, 11, 20 both upon 405 LED and sunlight irradiation are gathered in Table 4, and the results are fully accordance with existed literature data.<sup>48, 49</sup>

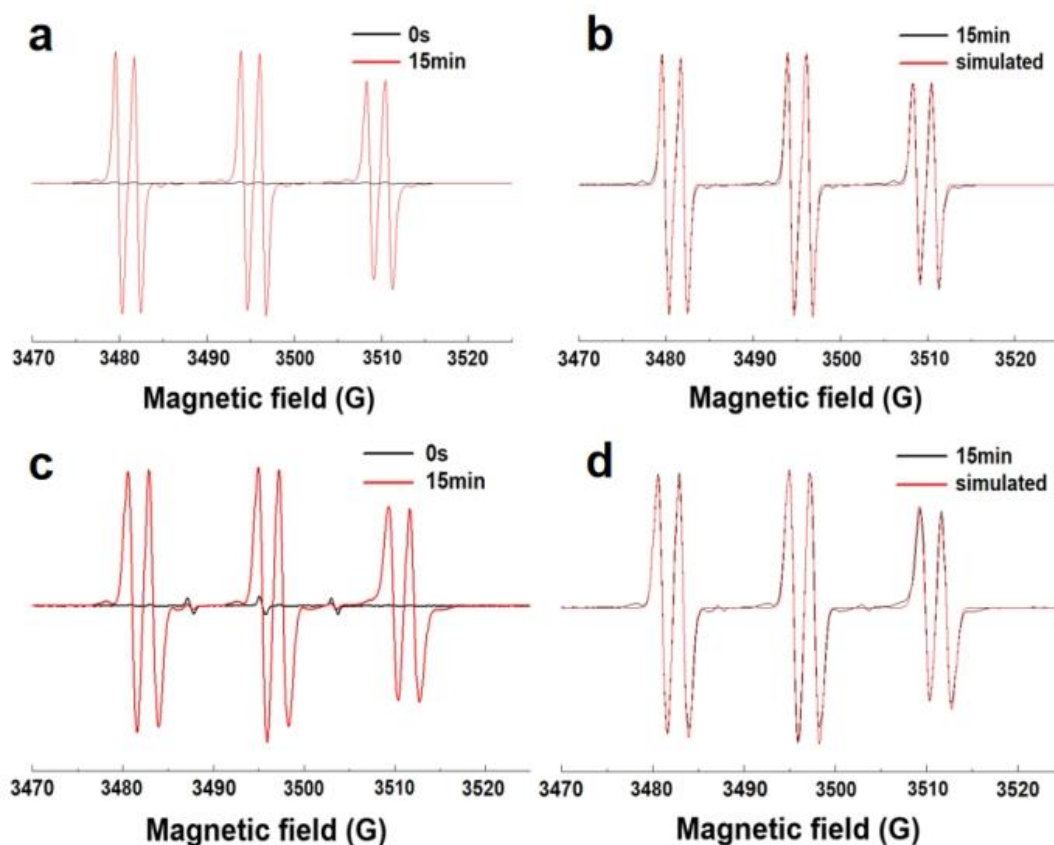


**Figure 11.** ESR spectra obtained from ESR-spin trapping experiments under irradiation of sunlight using PBN = 2 mg/mL (as the spin trap agent); Iod = 2 mg/mL, EDB = 2 mg/mL and dye 20 = 0.2 mg/mL in *tert*-butylbenzene under N<sub>2</sub>. (a) dye 20/Iod PIS, Irradiation time = 20min (green) = 10min (red) and = 0min (black) spectra, respectively; (b) dye 20/Iod PIS, Irradiation time = 20min experimental (black) and simulated (red) spectra; (c) dye 20/EDB PIS, Irradiation time = 10min (red) and = 0min (black) spectra; (d) dye 20/EDB PIS, Irradiation time = 10min experimental (black) and simulated (red) spectra.

**Table 4.** HFC constants determined by ESR-spin experiments for the dyes 7, 9, 11, 20 upon 405 nm LED or sunlight irradiation.

	Dye 7 405nm LED	Dye 9 405nm LED	Dye 11 at sunlight	Dye 20 405nm LED	Dye 20 sunlight
Dye/Iod	a <sub>N</sub> =14.4 a <sub>H</sub> =2.1	a <sub>N</sub> =14.4 a <sub>H</sub> =2.1	a <sub>N</sub> =14.4 a <sub>H</sub> =2.4	a <sub>N</sub> =14.2 a <sub>H</sub> =2.1	a <sub>N</sub> =14.4 a <sub>H</sub> =2.2
Dye/EDB	a <sub>N</sub> =14.4 a <sub>H</sub> =2.2	a <sub>N</sub> =14.4 a <sub>H</sub> =2.1	a <sub>N</sub> =14.4 a <sub>H</sub> =2.4	a <sub>N</sub> =14.4 a <sub>H</sub> =2.1	a <sub>N</sub> =14.4 a <sub>H</sub> =2.3

### 3.4. Direct laser write (DLW) experiments.

According to the excellent photoinitiation abilities of the investigated push-pull dyes, the DLW experiments were applied for the photopolymerization of TMPTA in the presence of dye-based PISs comprising dyes 7, 9 and 11. Here in this part, the compositions and concentrations of dyes 7, 9 and 11/Iod/EDB (0.1%/2%/2% in monomer, w/w/w) are the same as the sets used before. As expected, the 3D patterns (“LZ” for dye 7, “CD” for dye 9, “YR” for dye 11) were successfully produced in a very short time. After DLW experiments, profilometric observations were performed by numerical optical microscopy and smooth surfaces and excellent spatial resolution were found on these 3D profiles as well (See Figure 12). Here, the success of the DLW experiments strongly support the conclusion that the investigated push-pull dyes possess remarkable high light absorption and exhibited excellent photoinitiation abilities during the FRP process as aforementioned.

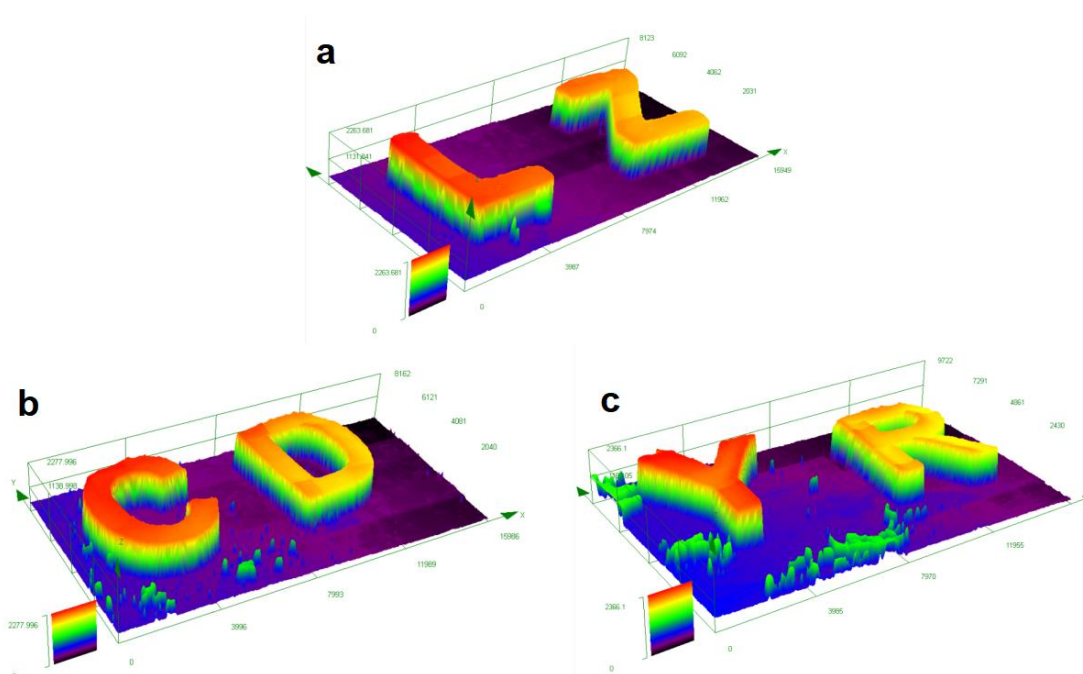


**Figure 12.** Free radical photopolymerization experiments for direct laser write (DLW) initiated by push-pull dye 7 based three-component photoinitiating systems in TMPTA. Characterization of the 3D patterns by numerical optical microscopy: 3-D overall



appearance of color pattern of dye/Iod/EDB (0.1%/2%/2% w/w/w) in TMPTA: **(a)** for dye 7/Iod/EDB; **(b)** for dye 9/Iod/EDB; **(c)** for dye 11/Iod/EDB.

### 3.5. Direct laser write (DLW) experiments for the photocomposites with silica fillers.

Similar to the previous part, photocomposites were prepared by DLW experiments by adding silica powders as fillers into monomer (TMTPA) and by using the dye 7, 9, 11-based PISs. Here, we set a weight ratio of 20% to monomer for silica powders and the compositions and concentrations of PISs are the same than for the DLW experiments without filler. However, because of the significant obstruction to the penetration of the laser light originating from silica fillers exhibiting a poor transmittance, a lower spatial resolution on 3D profiles of the resulting photocomposites were observed by numerical optical microscopy (“RUY” for dye 7/silica, “SAQ” for dye 9/silica, “HUI” for dye 11/silica, see Figure 13), compared to three selected dye-based PISs without fillers during DLW experiments. Even if photocomposites with silica fillers exhibited poorer photopolymerizable properties from the results, there is no doubt that the resulting composites can be regarded as useful photochemical materials for various research fields, e.g. photocuring, additive manufacturing or vat photopolymerization, etc.

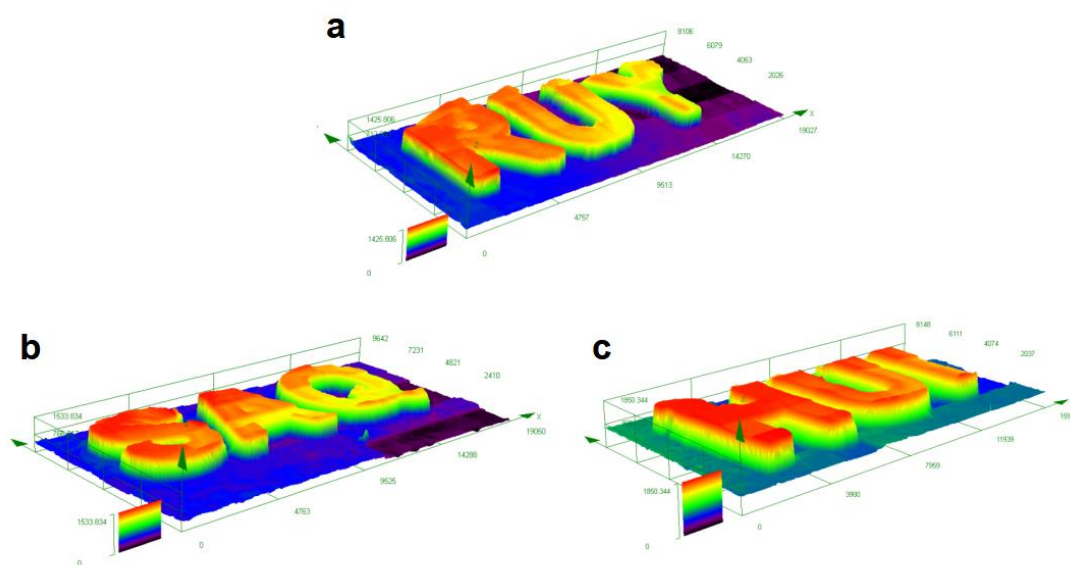


**Figure 13.** Free radical photopolymerization experiments in DLW experiments in TMPTA. Characterization of 3D overall appearance of 3D color patterns by numerical optical microscopy in the presence of: **(a)** dye 7/Iod/EDB/silica (0.1%/2%/2%/20% in TA, w/w/w/w); **(b)** dye 9/Iod/EDB/silica (0.1%/2%/2%/20% in TMPTA, w/w/w/w); **(c)** dye 11/Iod/EDB/silica (0.1%/2%/2%/20% in TMPTA, w/w/w/w).

#### 4. Conclusion

In this article, 25 novel organic chromophores were designed and synthesized to act as visible light photosensitizers. After the investigation of these two series of dyes, their push-pull structures proved to play a key-role, which contributed to their photoinitiation performances in free radical polymerization. More precisely, their high light absorption properties and photoinitiation abilities were examined by UV-vis spectroscopy and RT-FTIR experiments, respectively. Furthermore, six selected dyes were not only used as photoinitiators upon irradiation of 405 nm LED, their capable photoinitiation abilities were also exhibited efficiently during the polymerization process upon sunlight irradiation. Then, the supposed photochemical mechanism occurred in FRP process were investigated via steady state photolysis and fluorescence approaches, and the generated radicals were confirmed by ESR experiments. DLW experiments were performed to broaden the scope of applications of the newly developed photoinitiators, not only used on monomer with three-component PISs containing selected dyes, but also in the case of the polymerizable materials in the presence of silica fillers. Fortunately, 3D patterns were successfully obtained by polymerizing the monomer by using three-component PISs, even if in the presence of silica fillers (light penetration issue), indicating the feasible possibility by using the photocomposites to expand the knowledge of photochemistry in the future.

**Supplementary Materials: Figure S1.** Chemical structures of dye 14-25 used in this study; **Figure S2.** UV-vis absorption spectra of dyes 7; **Figure S3.** UV-vis absorption spectra of dyes 14, 15, 20; **Figure S4.** Cyclic voltammograms for the dyes 7, 9, 11 **Figure S5.** ESR spectra of dye 7 obtained from ESR-spin trapping experiment at 405nm LED; **Figure S6.** ESR spectra of dye 9 obtained from ESR-spin trapping experiment at 405nm LED; **Figure S7.** ESR spectra of dye 20 obtained from ESR-spin trapping

experiment at 405 nm LED; **Figure S8**. The Shortcuts of weather and address of experiments performed for sunlight irradiation.

**Funding:** The Agence Nationale de la Recherche (ANR agency) is acknowledged for funding through the PhD grant of Corentin Pigot (ANR-17-CE08-0010 DUALITY project).

**Acknowledgments:** Authors wish to thank the Region Grand Est (France) for the grant “MIPPI-4D”. PX acknowledges funding from the “Australian Research Council (FT170100301)”. This work was granted access to the HPC resources of the Mesocentre of the University of Strasbourg.

**Conflicts of Interest:** The authors declare no conflict of interest.

## References

(1) Liu, S.; Brunel, D.; Sun, K.; Zhang, Y.; Chen, H.; Xiao, P.; Dumur, F.; Lalevée, J. Novel photoinitiators based on benzophenone-Triphenylamine hybrid structure for LED photopolymerization. *Macromolecular Rapid Communications* **2020**, *41*(23), 2000460.

(2) Chen, H.; Noirbent, G.; Liu, S.; Brunel, D.; Graff, B.; Gigmes, D.; Zhang, Y.; Sun, K.; Morlet-Savary, F.; Xiao, P.; Dumur, F.; Lalevée, J. Bis-chalcone derivatives derived from natural products as near-UV/visible light sensitive photoinitiators for 3D/4D printing. *Materials Chemistry Frontiers* **2021**, *5*(2), 901-916.

(3) Liu, S.; Chen, H.; Zhang, Y.; Sun, K.; Xu, Y.; Morlet-Savary, F.; Graff, B.; Noirbent, G.; Pigot, C.; Brunel, D.; Nechab, M.; Gigmes, D.; Xiao, P.; Dumur, F.; Lalevée, J. Monocomponent photoinitiators based on benzophenone-carbazole structure for led photoinitiating systems and application on 3D printing. *Polymers* **2020**, *12*(6), 1394.

(4) Liu, S.; Brunel, D.; Sun, K.; Xu, Y.; Morlet-Savary, F.; Graff, B.; Xiao, P.; Dumur, F.; Lalevée, J. A monocomponent bifunctional benzophenone-carbazole type II photoinitiator for LED photoinitiating systems. *Polymer Chemistry* **2020**, *11*(21), 3551-3556.

(5) Sun, K.; Xu, Y.; Dumur, F.; Morlet-Savary, F.; Chen, H.; Dietlin, C.; Graff, B.; Lalevée, J.; Xiao, P. In silico rational design by molecular modeling of new ketones as photoinitiators in three-component photoinitiating systems: application in 3D printing. *Polymer Chemistry* **2020**, *11*(12), 2230-2242.

(6) Tehfe, M. A.; Dumur, F.; Graff, B.; Morlet-Savary, F.; Fouassier, J. P.; Gigmes, D.; Lalevée, J. New Push-Pull Dyes Derived from Michler's Ketone For Polymerization Reactions Upon Visible Lights. *Macromolecules* **2013**, *46*(10), 3761-3770.

(7) Tehfe, M. A.; Dumur, F.; Graff, B.; Morlet-Savary, F.; Gigmes, D.; Fouassier, J. P.; Lalevée, J. Push-pull (thio) barbituric acid derivatives in dye photosensitized

radical and cationic polymerization reactions under 457/473 nm laser beams or blue LEDs. *Polymer Chemistry* 2013, 4(13), 3866-3875.

(8) Tehfe M. A.; Dumur, F.; Graff, B.; Morlet-Savary, F.; Gigmes, D.; Fouassier, J. P.; Lalevée, J. New push-pull dyes derived from Michler's ketone for polymerization reactions upon visible lights. *Macromolecules* 2013, 46(10), 3761-3770.

(9) Xiao, P.; Frigoli, M.; Dumur, F.; Graff, B.; Gigmes, D.; Fouassier, J. P.; Lalevée, J. Julolidine or fluorenone based push-pull dyes for polymerization upon soft polychromatic visible light or green light. *Macromolecules* 2014, 47(1), 106-112.

(10) Noirbent, G.; Dumur, F. Recent advances on nitrofluorene derivatives: Versatile electron acceptors to create dyes absorbing from the visible to the near and far-infrared region. *Materials* 2018, 11(12), 2425.

(11) Blanchard-Desce, M.; Wortmann, R.; Lebus, S.; Lehn, J. M.; Krämer, P. Intramolecular charge transfer in elongated donor-acceptor conjugated polyenes. *Chem. Phys. Lett.* 1995, 243(5-6), 526-532.

(12) Noirbent, G.; Pigot, C.; Bui, T.-T.; Peralta, S.; Nechab, M.; Gigmes, D.; Dumur, F. Synthesis, optical and electrochemical properties of a series of push-pull dyes based on the 2-(3-cyano-4,5,5-trimethylfuran-2(5H)-ylidene) malononitrile (TCF) acceptor, *Dyes and Pigments* 2021, 184, 108807.

(13) Pigot, C.; Noirbent, G.; Peralta, S.; Duval, S.; Nechab, M.; Gigmes, D.; Dumur, F. Unprecedented Nucleophilic Attack of Piperidine on the Electron Acceptor during the Synthesis of Push-Pull Dyes by a Knoevenagel Reaction. *Helv. Chim. Acta* 2019, 102, e1900229.

(14) Turkoglu, G.; Cinar, M.E.; Ozturk, T. Triarylborane-based materials for OLED applications. *Molecules* 2017, 22(9), 1522.

(15) Paek, S.; Lee, J.K.; Ko, J. Synthesis and photovoltaic characteristics of push-pull organic semiconductors containing an electron-rich dithienosilole bridge for solution-processed small-molecule organic solar cells. *Sol. Energ. Mater. Solar Cells* 2014, 120, 209-217.

(16) Xu, S. J.; Zhou, Z.; Liu, W.; Zhang, Z.; Liu, F.; Yan, H.; Zhu, X. A twisted thieno[3,4-*b*]thiophene-based electron acceptor featuring a 14- $\pi$ -electron indenoindene core for high-performance organic photovoltaics. *Adv. Mater.* 2017, 29(43), 1704510.

(17) Karak, S.; Liu, F.; Russell, T.P.; Duzhko, V.V. Bulk charge carrier transport in push-pull type organic semiconductor. *ACS Appl. Mater. Interfaces* 2014, 6(23), 20904–20912.

(18) Raimundo, J.M.; Blanchard, P.; Gallego-Planas, N.; Mercier, N.; Ledoux-Rak, I.; Hierle, R.; Roncali, J. Design and synthesis of push-pull chromophores for second-order nonlinear optics derived from rigidified thiophene-based  $\pi$ -conjugating spacers. *J. Org. Chem.* 2002, 67(1), 205–218.

(19) El-Shishtawy, R. M.; Borbone, F.; Al-amshany, Z. M.; Tuzi, A.; Barsella, A.; Asiri, A. M.; Roviello, A. Thiazole azo dyes with lateral donor branch: Synthesis, structure and second order NLO properties. *Dyes and Pigments.* 2013, 96(1), 45–51.

(20) Cesaretti, A.; Bonaccorso, C.; Elisei, F.; Fortuna, C. G.; Mencaroni, L.; Spalletti, A. Photoinduced Intramolecular Charge Transfer and Hyperpolarizability Coefficient in Push-Pull Pyridinium Salts with Increasing Strength of the Acceptor Group. *ChemPlusChem* 2018, 83(11), 1021-1031.

(21) Motiei, H.; Jafari, A.; Naderali, R. Third-order nonlinear optical properties of organic azo dyes by using strength of nonlinearity parameter and Z-scan technique. *Optics & Laser Technology* 2017, 88, 68-74.

(22) El-Shishtawy, R. M.; Al-Zahrani, F. A.; Afzal, S. M.; Razvi, M. A. N.; Al-amshany, Z. M.; Bakry, A. H.; Asiri, A. M. Synthesis, linear and nonlinear optical properties of a new dimethine cyanine dye derived from phenothiazine. *RSC advances* 2016, 6(94), 91546-91556.

(23) Gao, S. H.; Xie, M. S.; Wang, H. X.; Niu, H. Y.; Qu, G. R.; Guo, H. M. Highly selective detection of Hg<sup>2+</sup> ion by push-pull-type purine nucleoside-based fluorescent sensor. *Tetrahedron* 2014, 70(33), 4929–4933.

(24) Sun, K.; Pigot, C.; Chen, H.; Nechab, M.; Gimes, D.; Morlet-Savary, F.; Graff, B.; Liu, S. Xiao, P.; Dumur, F.; Lalevée, J. Free radical photopolymerization and

3d printing using newly developed dyes: Indane-1, 3-dione and 1H-cyclopentanaphthalene-1, 3-dione derivatives as photoinitiators in three-component systems. *Catalysts* 2020, 10(4), 463.

(25) Sun, K.; Liu, S.; Pigot, C.; Brunel, D.; Graff, B.; Nechab, M.; Gigmes, D.; Morlet-Savary, F.; Zhang, Y. Xiao, Pu.; Dumur, F.; Lalevée, J. Novel Push–Pull Dyes Derived from 1H-cyclopenta [b] naphthalene-1, 3 (2H)-dione as Versatile Photoinitiators for Photopolymerization and Their Related Applications: 3D Printing and Fabrication of Photocomposites. *Catalysts* **2020**, 10(10), 1196.

(26) Sun, K.; Liu, S.; Chen, H.; Morlet-Savary, F.; Graff, B.; Pigot, C.; Nechab, M.; Xiao, P.; Dumur, F.; Lalevée, J. N-ethyl Carbazole-1-Allylidene-Based Push-Pull Dyes as Efficient Light Harvesting Photoinitiators for Sunlight Induced Polymerization. *European Polymer Journal* **2021**, 110331.

(27) Sun, K.; Chen, H.; Zhang, Y.; Morlet-Savary, F.; Graff, B.; Xiao, P.; Dumur, F.; Lalevée, J. High-performance Sunlight Induced Polymerization Using Novel Push-Pull Dyes with High Light Absorption Properties. *European Polymer Journal* **2021**, 110410.

(28) Diffey, B.; Osterwalder, U. Labelled sunscreen SPFs may overestimate protection in natural sunlight. *Photochemical & Photobiological Sciences* **2017**, 16(10), 1519-1523.

(29) Fouassier, J. P.; Allonas, X.; Burget, D. Photopolymerization reactions under visible lights: principle, mechanisms and examples of applications. *Progress in organic coatings* **2003**, 47(1), 16-36.

(30) Allegrezza, M. L.; DeMartini, Z. M.; Kloster, A. J.; Digby, Z. A.; Konkolewicz, D. Visible and sunlight driven RAFT photopolymerization accelerated by amines: kinetics and mechanism. *Polymer Chemistry* 2016, 7(43), 6626-6636.

(31) Wang, J.; Rivero, M.; Muñoz Bonilla, A.; Sanchez-Marcos, J.; Xue, W.; Chen, G.; Zhang, W.; Zhu, X. Natural RAFT polymerization: recyclable-catalyst-aided, opened-to-Air, and sunlight-photolyzed RAFT polymerizations. *ACS Macro Letters* 2016, 5(11), 1278-1282.

(32) Ciftci, M.; Tasdelen, M. A.; Yagci, Y. Sunlight induced atom transfer radical polymerization by using dimanganese decacarbonyl. *Polymer Chemistry* 2014, 5(2), 600-606.

(33) Decker, C.; Bendaikha, T. Interpenetrating polymer networks. II. Sunlight-induced polymerization of multifunctional acrylates. *Journal of applied polymer science* 1998, 70(11), 2269-2282.

(34) Schmitt, M. Synthesis and testing of ZnO nanoparticles for photo-initiation: experimental observation of two different non-migration initiators for bulk polymerization. *Nanoscale* 2015, 7(21), 9532-9544.

(35) Dietlin, C.; Schweizer, S.; Xiao, P.; Zhang, J.; Morlet-savary, F.; Graff, B.; Fouassier, J. P.; Lalevée, J. Photopolymerization upon LEDs: new photoinitiating systems and strategies. *Polym. Chem.* **2015**, 6(21), 3895-3912.

(36) Lalevée, J.; Blanchard, N.; Tehfe, M.A.; Morlet-Savary, F.; Fouassier, J. P. Green bulb light source induced epoxy cationic polymerization under air using tris (2, 2'-bipyridine) ruthenium (II) and silyl radicals. *Macromolecules* **2010**, 43(24), 10191–10195.

(37) Lalevée, J.; Blanchard, N.; Tehfe, M.A.; Peter, M.; Morlet- Savary, F.; Gigmes, D.; Fouassier, J. P. Efficient dual radical/cationic photoinitiator under visible light: a new concept. *Polym. Chem.*, **2011**, 2(9), 1986–1991.

(38) Xu, Y. Y.; Ding, Z. F.; Liu, F. Y.; Sun, K.; Dietlin, C.; Lalevée, J.; Xiao, P. 3D Printing of Polydiacetylene Photocomposite Materials: Two Wavelengths for Two Orthogonal Chemistries. *ACS Applied Materials & Interfaces* **2019**, 12(1), 1658-1664.

(39) Rehm, D.; Weller, A. Kinetics of fluorescence quenching by electron and H-atom transfer. *Isr. J. Chem.* **1970**, 8(2), 259–271.

(40) Romanczyk, P. P.; Kurek, S. S. The Reduction Potential of Diphenyliodonium Polymerisation Photoinitiator Is Not  $-0.2$  V vs. SCE. A Computational Study *Electrochim. Acta* **2017**, 225, 482–485.

(41) Fouassier, J. P.; Lalevée, J. Photoinitiators for polymer synthesis – scope, reactivity, and efficiency. Weinheim: *John Wiley & Sons*, **2012**.



(42) James, B.; Frisch, A. Exploring chemistry with electronic structure methods. *Gaussian, Incorporated*, **1996**.

(43) Frisch, M. J.; Trucks, G. W.; Schlegel, H. B.; Scuseria, G. E.; Robb, M. A.; Cheeseman, J. R.; Zakrzewski, V. G.; Montgomery, J. A.; Stratmann, R. E.; Burant, J. C.; Dapprich, S.; Millam, J. M.; Daniels, A. D.; Kudin, K. N.; Strain, M. C.; Farkas, O.; Tomasi, J.; Barone, V.; Cossi, M.; Cammi, R.; Mennucci, B.; Pomelli, C.; Adamo, C.; Clifford, S. J.; Ochterski, W.; Petersson, G. A.; Ayala, P. Y.; Cui, Q.; Morokuma, K.; Salvador, P.; Dannenberg, J. J.; Malick, D. K.; Rabuck, A. D.; Raghavachari, K.; Foresman, J. B.; Cioslowski, J.; Ortiz, J. V.; Baboul, A. G.; Stefanov, B. B.; Liu, G.; Liashenko, A.; Piskorz, P.; Komaromi, I.; Gomperts, R.; Martin, R. L.; Fox, D. J.; Keith, T.; Al-Laham, M. A.; Peng, C. Y.; Nanayakkara, A.; Challacombe, M.; Gill, P. M. W.; Johnson, B.; Chen, W.; Wong, M. W.; Andres, J. L.; Gonzalez, C.; Head-Gordon, M.; Replogle, E. S.; Pople, J. A. *Gaussian 03, Revision B-2*, Gaussian Inc., Pittsburgh, PA, **2003**.

(44) Bureš, F. Fundamental Aspects of Property Tuning in Push–Pull Molecules. *RSC Adv.* **2014**, *4* (102), 58826–58851.

(45) Pigot, C.; Noirbent, G.; Peralta, S.; Duval, S.; Bui, T.-T.; Aubert, P.-H.; Nechab, M.; Gigmes, D.; Dumur, F. New push-pull dyes based on 2-(3-oxo-2,3-dihydro-1*H*-cyclopenta[*b*]naphthalen-1-ylidene)malononitrile: An amine-directed synthesis. *Dyes Pigm.* **2020**, *175*, 108182.

(46) Pigot, C.; Noirbent, G.; Peralta, S.; Duval, S.; Nechab, M.; Gigmes, D.; Dumur, F. Unprecedented nucleophilic attack of piperidine on the electron acceptor during the synthesis of push-pull dyes by a Knoevenagel reaction. *Helv. Chim. Acta* **2019**, *102*, e1900229.

(47) Sun, K.; Xiao, Pu; Dumur, F.; Lalevée, J. Organic dye-based photoinitiating systems for visible-light-induced photopolymerization. *J. Polym. Sci.* **2021**.

(48) Haire, L.D.; Krygsmann, P.H.; Janzen, E.G.; Oehler, U.M. Correlation of radical structure with EPR spin adduct parameters: utility of the proton, carbon-13, and nitrogen-14 hyperfine splitting constants of aminoxyl adducts of PBN-nitronyl-<sup>13</sup>C for

three-parameter scatter plots. *J. Org. Chem.* 1988, 53, 4535-4542.

(49) Ohto, N.; Niki, E.; Kamiya, Y. Study of autoxidation by spin trapping. Spin trapping of peroxy radicals by phenyl N-t-butyl nitron. *J. Chem. Soc., Perkin Trans. 2*, 1977, 13, 1770-1774.

TOC Graphic:



## Sunlight Induced Polymerization

